skaderisiko-

analyse

Lars Gottschalk og Irina Krasovskaia

Economic Risk of Flooding – a case study for the flood-plain upstream Nor in the Glomma River, Norway

R

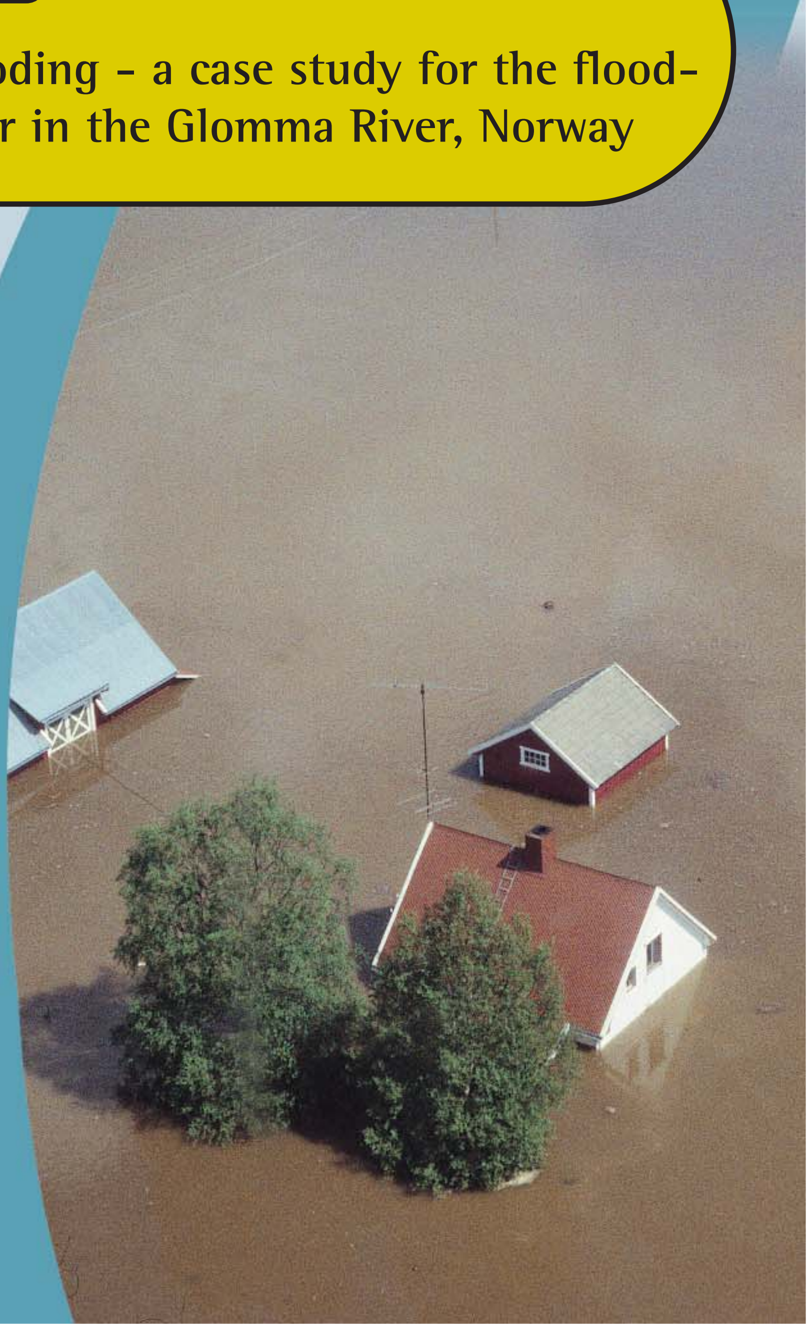

HYDRA - et forskningsprogram om flom

HYDRA er et forskningsprogram om flom initiert av Norges vassdrags- og energidirektorat (NVE) i 1995. Programmet har en tidsramme på 3 år, med avslutning medio 1999, og en kostnadsramme på ca. 18 mill. kroner. HYDRA er i hovedsak finansiert av Olje- og energidepartementet.

Arbeidshypotesen til HYDRA er at summen av alle menneskelige påvirkninger i form av arealbruk, reguleringer, forbygningsarbeider m.m. kan ha økt risikoen for flom.

Målgruppen for HYDRA er statlige og kommunale myndigheter, forsikringsbransjen, utdannings- og forskningsinstitusjoner og andre institusjoner. Nedenfor gis en oversikt over fagfelt/tema som blir berørt i HYDRA:

- **Naturgrunnlag og arealbruk**
- **Skaderisikoanalyse**
- **Tettsteder**
- **Miljøvirkninger av flom og flomforebyggende tiltak**
- **Flomdemping, flomvern og flomhandtering**
- **Databaser og GIS**
- **Modellutvikling**

Sentrale aktører i HYDRA er; Det norske meteorologiske institutt (DNMI), Glommens og Laagens Brukseierforening (GLB), Jordforsk, Norges geologiske undersøkelse (NGU), Norges Landbrukshøgskole (NLH), Norges teknisk-naturvitenskapelige universitet (NTNU), Norges vassdrags- og energidirektorat (NVE), Norsk institutt for jord- og skogkartlegging (NIJOS), Norsk institutt for vannforskning (NIVA), SINTEF, Stiftelsen for Naturforskning og Kulturminneforskning (NINA/NIKU) og universitetene i Oslo og Bergen.

HYDRA - a research programme on floods

HYDRA is a research programme on floods initiated by the Norwegian Water Resources and Energy Directorate (NVE) in 1995. The programme has a time frame of 3 years, terminating in 1999, and with an economic framework of NOK 18 million. HYDRA is largely financed by the Ministry of Petroleum and Energy.

The working hypotesis for HYDRA is that the sum of all human impacts in the form of land use, regulation, flood protection etc., can have increased the risk of floods.

HYDRA is aimed at state and municipal authorities, insurance companies, educational and research institutions, and other organization.
An overview of the scientific content in HYDRA is:

- **Natural resources and land use**
- **Risk analysis**
- **Urban areas**
- **Flood reduction, flood protection and flood management**
- **Databases and GIS**
- **Environmental consequences of floods and flood prevention measures**
- **Modelling**

Central institutions in the HYDRA programme are; The Norwegian Meteorological Institute (DNMI), The Glommens and Laagens Water Management Association (GLB), Centre of Soil and Environmental Research (Jordforsk), The Norwegian Geological Survey (NGU), The Agriculture University of Norway (NLH), The Norwegian University of Science and Technology (NTNU), The Norwegian Water Resources and Energy Directorate (NVE), The Norwegian Institute of Land Inventory (NIJOS), The Norwegian Institute for Water Research (NIVA), The Foundation for Scientific and Industrial Research at the Norwegian Institute of Technology (SINTEF), The Norwegian Institute for Nature and Cultural Heritage Research (NINA/NIKU) and the Universities of Oslo and Bergen.

HYDRA-rapport nr. R01

Economic Risk of Flooding

- a case study for the floodplain upstream Nor in the Glomma River, Norway

by

Lars Gottschalk
Dept. of Geophysics, University of Oslo

Irina Krasovskaia
Dept. of Earth Sciences, Hydrology, University of Uppsala

Preface

The Risk Analysis Project of the HYDRA research programme has as its main objective to improve the methodology for flood loss assessment - aimed at streamlining cost/benefit analysis of flood mitigation measures. It has four main components:

- establishment of damage/loss functions (R1);
- improving flood mapping (R2);
- flood analysis and risk analysis (R3);
- improved front line decision tools (R4).

The third component is focusing on improving regional flood frequency analysis and flood line estimation, test and verification of loss curves and the establishment of frequency/damage curves. This report is a contribution to this third component with relevance for all these focal topics. A methodology for economic risk of flooding is developed and applied to the floodplains upstream Nor in the Glomma river.

Oslo, June 1999

Nils Roar Sælthun
Project Manager

Contents

Summary

The aim of this study has been to analyse factors influencing the risk of flooding and to develop a methodology for estimating this risk, i.e. establish a relation between the cost of damage caused by flooding and the probability of the flood. The method combines novel procedures for estimating a regional flood frequency curve as well as stage damage curves. The estimation of the regional flood frequency curve is based on a L-moment analysis including effects of scaling.

The stage damage curve estimation is based on statistical procedure for identifying the number of buildings (or other objects) flooded on a flood plain by a flood with a certain probability of exceedance and on cost of the damage for individual objects as a function of river stage. The method is applied to the Grue and Åsnes municipalities upstream Nor in the Glomma river. All data used in the study have been provided by the HYDRA project.

Sammendrag

Målet med denne undersøkelsen har vært å analysere faktorer som påvirker risikoen for oversvømmelse og å utvikle metoder for å estimere denne risikoen, dvs. å etablere en sammenheng mellom skadekostnadene forårsaket av en oversvømmelse og sannsynligheten for denne flommen. Metoden kombinerer nye prosedyrer for å estimere en regional flomfrekvenskurve og vannstand-skadekurver. Estimeringen av den regionale flomfrekvenskurven er basert på en analyse av L-moment, inkludert skalaeffekter. Estimatene av vannstand-skadekurvene er basert på statistisk prosedyrer for å identifisere antall bygninger (eller andre objekt) som blir oversvømmet på en elveslette ved en flom med en viss sannsynlighet for overskridelse, og på skadekostnadene for individuelle objekt som en funksjon av elvevannstand. Metoden er brukt i Grue og Åsnes kommuner oppstrøms Nor i Glomma. Alle data som ble brukt i denne undersøkelsen kommer fra HYDRA prosjektet.

1. Introduction

Leonardo da Vinci writes: ”Among unrestrainable and devastating visitations the flooding of the destructive rivers with no doubt must be placed before any other horror” (Codex Atlanticus 108 vb) (Fig. 1). 500 years later the flooding of the rivers continues to be a major threat to life and property. A number of extreme hydrological events of exceptional severity makes many believe that the threats are greater today than ever before. It is clear that many floods have occurred during the 1980s and 1990s world wide (WMO, 1995). Floods (and drought) cause more damage and kill more people than any other natural disaster (Rodda, 1995). Kundzewics (1998) gives a spectacular overview of floods during the 1990s which makes one wonder if it really was as bad as that before. We can only speculate whether Leonardo would have agreed that the situation has become worse through the centuries. In what way has the situation become worse? Is it so that the extreme events causing flooding are getting more frequent and have higher magnitude? Or is it so that the devastating consequences of flooding become more and more spectacular attracting large attention, not because of increased floods, but because the vulnerability of our society to floods has increased?

The frequency of an undesirable event and a measure of the severity of adverse effects of it (Lowrance, 1976) or the danger that undesirable events represent to human beings, the environment and economic values (Aven, 1992) are both parts of the concept of risk. From this point of view it can be stated that the risk for flooding has increased. There is probably a general consensus around this statement. The reason why it has increased is a more controversial question and it is not possible to give some general statement on this. The individual conditions for each country or even drainage basin give different answers to this question. Here we will try to identify factors that determine the risk of flooding and develop a risk model for the Glomma River. This model is applied to the Grue and Åsnes (Fig. 2) municipalities upstream Nor in the Glomma river (Fig. 3).

Figure 1. Drawing by Leonardo da Vinci showing a mountain chain opened by flooding water and causing landslides. The drawing might be inspired by the Bellinzona catastrophe in 1515 referenced in the literature. A parallel to this event, but less disastrous, is the flooding in Posciavo in 1993.

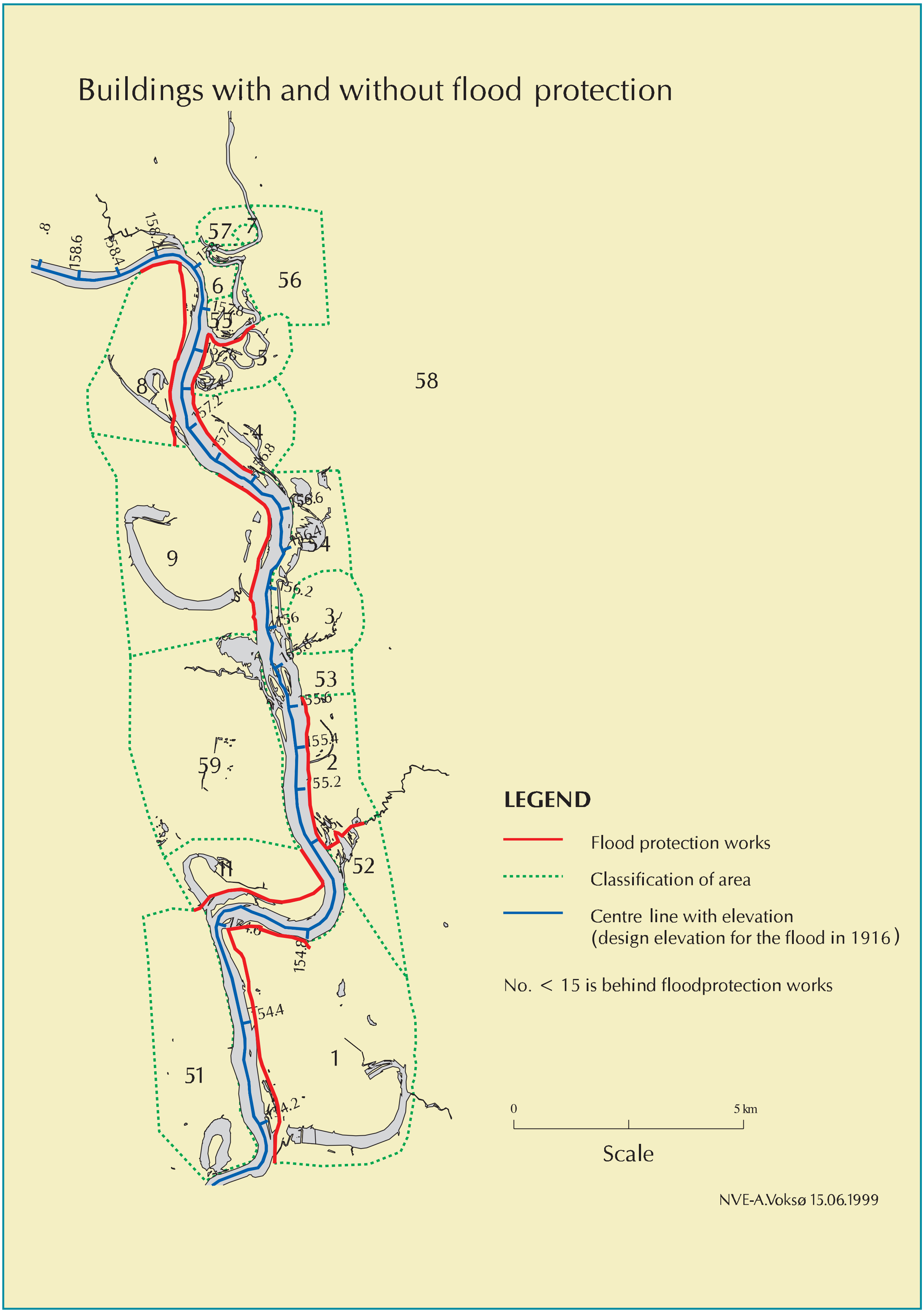

Figure 2. Situation map along the Glomma river at Grue and Åsnes municipalities. 18 settlement clusters are identified. Eight of these clusters are protected by dikes (bold lines).

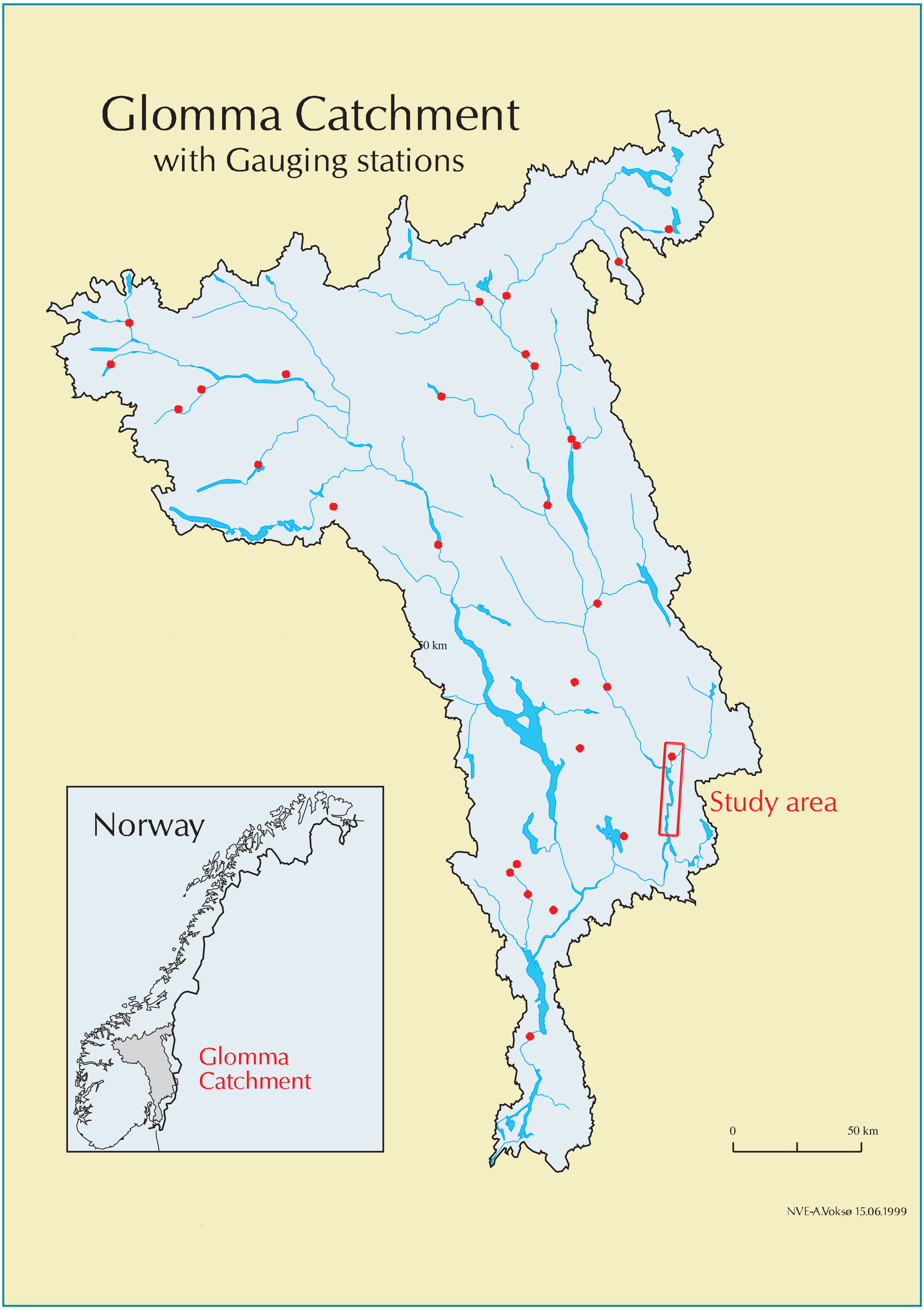

Figure 3. The Glomma drainage basin with hydrological gauging stations. The study area around Grue and Åsnes municipalities is marked by a rectangle.

2. Factors influencing the risk of flooding

Hydrologist, by tradition, had a rather narrow perspective on extreme flood events defining the probability for such events to occur, usually in terms of its return period. Only recently the risk concept has come into focus including as well the measure of probability as some estimate of consequences. It has to be admitted that there is a confusion in the use of the concept of risk in the hydrologic literature. Yevjevich (1977) was the first to express this ambiguity. At least three interpretations can be found. Risk can be equal to the probability of exceedance of a certain flood level within a given design period (Haan, 1977, Kite 1977). A more common interpretation is the probability of failure of a system (storm sewer networks, flood dikes, bridges) with consideration of all uncertainties involved in the estimation of this (Tang et al. 1975, Simonovic and Mariño 1981, Tung and Mays 1981, Jain et al. 1992, Plate 1998). Many of the quoted works at the same time define the expected damage or the expected loss as a separate concept. Plate (1998) calls this the generalized risk. Finally, a more generally accepted definition of risk as the expected loss, damage or utility (Berger, 1985, Aven, 1992, Norsk Standard NS 5814) is also used in hydrologic applications (Ashkar and Rouselle 1981, Mitsiopulos et al. 1991, Lambert and Li 1994, Thompson 1997, Steadinger 1997). It should be noted that uncertainty is an important issue also in this definition of the risk concept (see 3 below). Herein only this latter definition will be used. Below a review of factors that influence this risk is given.

In the North American hydrologic literature flood damage is a central topic. James and Hall (1986) recall the development in the United States. Tremendous efforts have been made to lower these damages since the start in 1936 of a program to contain floods by constructing dams, dikes and channels. In 1966, it is noted that the national damage totals continue to rise and a new type of disasters appear namely, the failure of protective structures. In 1986 the damage totals are still rising. A new cost is introduced - loss of economic productivity of floodplain land. The program of measures for reducing flood damage in the US also contains delineation of areas subject to inundation on flood insurance rate maps (FIRM) showing 100-year and 500-year floodplain boundaries. A flood hazard factor is defined as the difference between the 10-year and 100-year flood water-surface elevation.

Handmer (1983), in a commentary to the paper by James and Hall, criticizes their general conclusion that the cause for the continuing rise in flood damage is mainly to seek in a failure to inform about the 100-year flood standard. Information cannot solve the problem, as people do not have a free choice where to settle. He instead gives the following three reasons for rising damage trends:

1. Increased floodplain investment results from encroachment onto floodplains and intensification of existing development, as well as from changes to the content of the buildings. Both the value of property at risk and its susceptibility to flood damages may be affected.

2. Geophysical factors include climatic change or variability, land subsidence, and stream channel change.

3. Better reporting of damages might also be stimulated by the availability of insurance with subsidized premiums.

Handmer concludes his discussion by referring to the fact that in New South Wales, Australia the 100 year standard has been abandoned in favour of an approach based on the hazard (water depth and velocity), economic, social, and environmental aspects of each development proposal. This change in approach is similar to the experience from Switzerland. A new policy in design flood protection schemes has been developed as a consequence of the severe damage by the floods in the Reuss and Poschiavo valleys in the Swiss Alps in 1987 (Jaeggi and Zarn, 1990). Extreme flooding is defined from the combined action of flow velocity and depth. The design principles are dependent on the type of objects to be protected and landscape/land-use classes.

A method for coping with the problem of flooding - ”Inondabilité” has been developed in France. Its aim is to couple the ”obvious social demand for protection against inundation and the knowledge which may exist on the hydrological and hydraulic functioning of drainage basins and river channels” (Gilard, 1998). The different components of the method are illustrated in Fig. 4. The point of departure for this method is not only the frequency of occurrence of extreme floods but also their duration and depth (which allows the calculation of velocities) coinciding with the experiences from Australia and Switzerland quoted above. Each critical situation is thus characterized by a triplet (T - return period, d - duration, p - depth). This triplet describes the random nature of the runoff formation processes (”aléa”). The methodology for establishing this triplet for

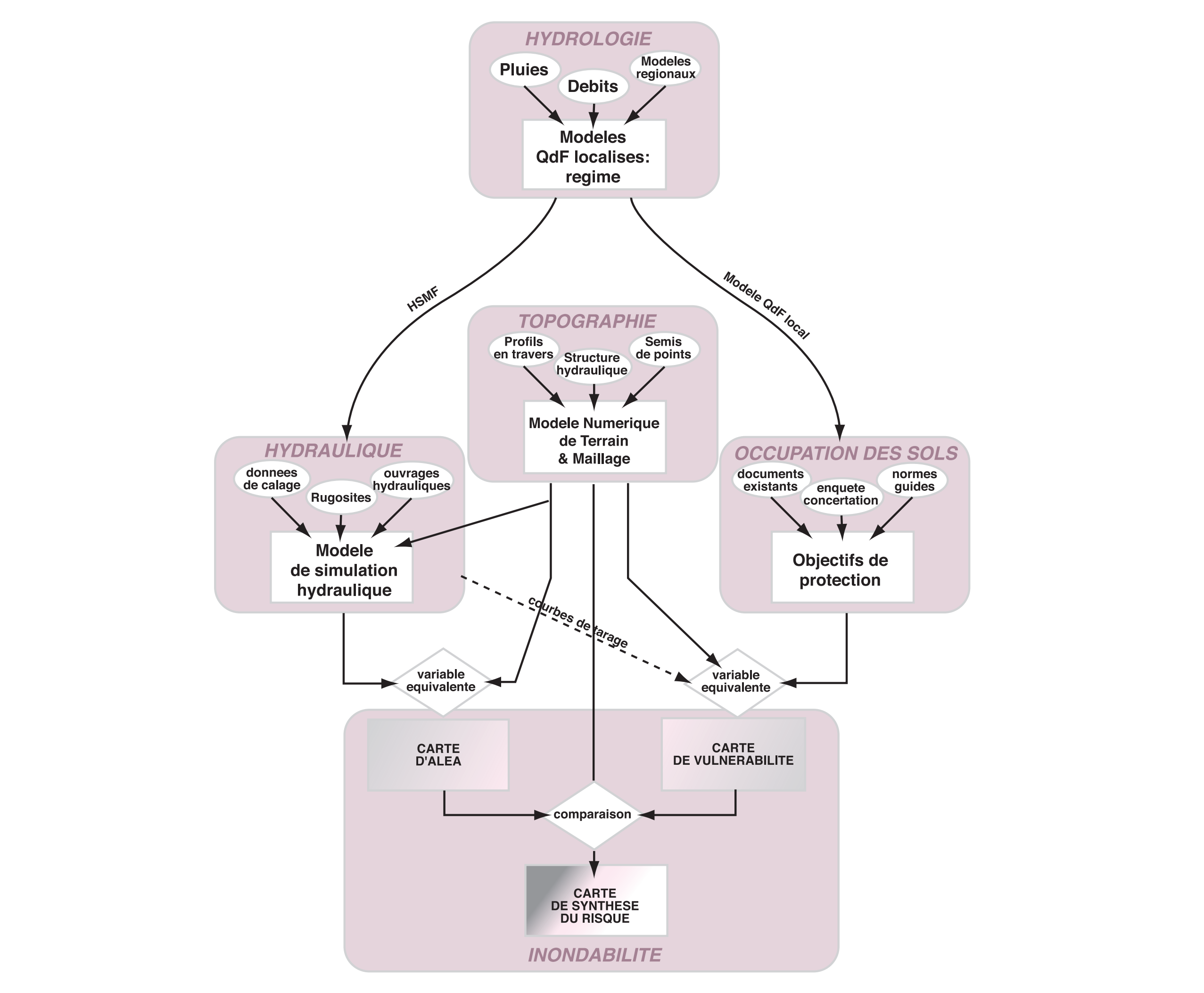

Figure 4. The components for flood risk mapping in France by the method "Inondabilité" (from Gilard, 1998).

a certain site from single site or regional analysis of runoff data is named QdF (Q -discharge, d -duration, F-frequency) (Galea and Prudhomme, 1994).

The vulnerability ("vulnerabilité") is the other important matching component to the "aléa" of this method. It is based on the concept of maximal acceptable risk (RXA). It is claimed that the definition of risk as the expected damage is impossible to apply in the practical situation. The damage of flooding is dependent on a multitude of factors and all of these cannot be meaningfully related to only the frequency of extreme discharge (extreme water level). The RXA is the alternative and it can be established for each type of landuse class in terms of a triplet (T,d,p) (Fig. 5) (Desbos, 1995). A critical point in this approach is the recalculation of triplets into an equivalent vulnerability in accordance with the relation: (T, d, p) → (T, 0, 0) to be able to conform different landuse to one comparable value. This recalculation contains several subjective assumptions of how RXA are related without any explicit specification of these. Finally the equivalent vulnerability is confronted with the corresponding "aléa" for a certain land area. Three situations may appear - i) the "aléa" is negligible, ii) the "aléa" is less than the vulnerability, and iii) the vulnerability exceeds the "aléa". Maps containing these three categories are produced.

Burrell and Keefe (1989), Watt and Paine (1992), and Paine and Watt (1992) report on the experience of flooding and flood damage reduction efforts in Canada. A national flood damage reduction program was started in 1976, which initiated a large number of flood risk mapping projects. On a flood risk map a distinction is made between the "floodway" defined as the area delineated by the 20 year flood and the "flood risk area" related to the 100 year flood. The need for evaluating uncertainty is stressed due to the wide range in the quality of maps, the unacceptable high unit mapping cost for small areas and the fact that the total uncertainty may be too high for the intended use. The following uncertainties in the production of floodplain maps have been identified:

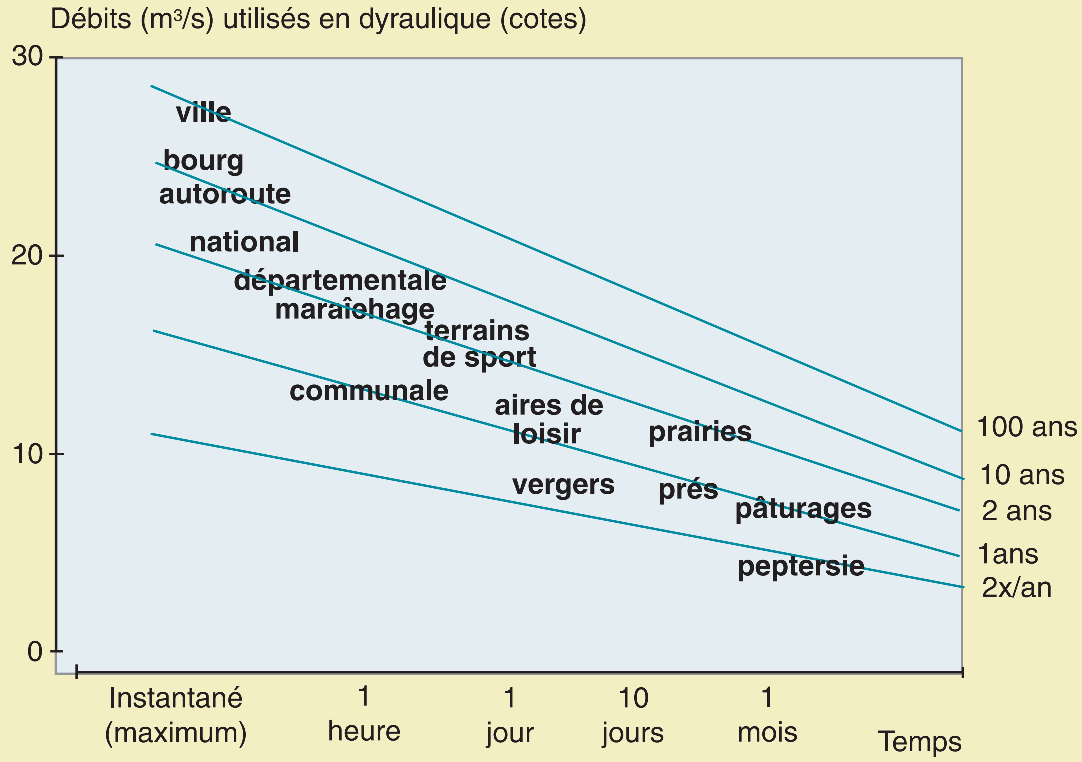

Figure 5. Example of vulnerability triplets (T, d, p) in graphical form for different landuse classes of the "Inondabilité" approach (Gilard, 1998).

1) topographic uncertainty;
2) hydrologic uncertainty;
   a) flood frequency analysis techniques (regional analysis);
   b) streamflow simulation techniques (use of conceptual models);
3) hydraulic uncertainty;
4) water surface elevation (depth) uncertainty;
5) uncertainty in depth of inundation.

A common conclusion is that the accuracy of design flows (hydrologic uncertainty) for each area exceeds other ones by a large margin, typically in the order of ±0.5 meters. Table 1 shows the two types of hydrologic uncertainty as evaluated by Watt and Paine (1992).

In Europe the devastating floods in the Rhein and Meuse basins in 1992, 1993 and 1996, in Po 1994 and in Odra/Oder 1997 have once more put the risk of flooding in the focus also in this part of the world.

Table 1: Hydrologic uncertainty (from Watt and Paine, 1992).

Criterion	Total hydrologic uncertainty [%]
Specified water level	0
Specified flow	0
100-year flood (regional analysis)	lesser of 25 or 5+65/÷N
100-year rain flood (calibrated model)	35
100-year rain flood (uncalibrated model)	50
100-year rain and snowmelt flood (calibrated model)	40
100-year rain and snowmelt flood (uncalibrated model)	55
Regional storm (uncalibrated model)	50

Other severe events were the flash floods in Vaison-la-Romaine, France in 1992 and in Posciavo, Switzerland in 1993. Several research projects have been launched coordinated by concerted actions like RIBAMOD and RIPARIUS (http://www.hrwallingford.co.uk/) and Flood Aware (http://wwwhh.lyon.cemagref.fr/floodaware). In Norway the flood in the Glomma River in 1995 initiated the HYDRA research program which is the background for this report. This river has earlier experienced severe flooding in 1773, 1789 (Storofsen), 1846, 1890, 1916, 1934, 1966, 1967 and recently in 1995 (Vesleofsen) (Fig. 6). The stress in the European efforts to cope with flooding is put on the human factor as the main cause for the increased flood risk manifested in a changing climate and changing environment (land use). For the HYDRA project the working hypothesis is that "the sum of all human impacts in the form of land use, regulation, flood-protection etc., may have increased the risk of floods".

There is already a vast literature on possible changes of runoff due to a changing climate. Krasovskaia (1996) and Gottschalk and Krasovskaia (1997) give extensive reviews related to Scandinavian conditions. In relation to floods, their conclusion is that the magnitude of individual floods is not influenced to any significant degree. On the other hand there is a tendency that that the number of flood events increases with increasing temperature in Southern Scandinavia. The overall effect of this is that the probability for extreme events slightly increases with a higher temperature. The fact that the number of flood events increased can mainly be interpreted so that weather systems (circulation patterns) giving rise to high precipitation over large areas become more frequent. This is in agreement with the conclusion by Caspary (1998) that the recent very high floods in the upper Danube and upper Rhine were caused by a change in prevailing tracks of weather systems over Northern Europe.

It is a common feature that floods are high over large territories at the same time. Quasi-periodic phenomena like the sunspot intensity (Yongquan, 1993) and recently the El Niño Southern Oscillation (ENSO) are possible causes behind such fluctuations in flood magnitudes and intensities. The signals are usually rather weak. This varies of cause with the geographical position. Krasovskaia et al. (1999) studying the ENSO influence on floods in Costa Rica found that also in this case the magnitude is almost constant while the frequency of events is strongly increasing during La Niña years connected to more frequent tropical storms. Hydrological design has traditionally been based on the assumption of stationarity. As formulated by Kuusisto et al. (1994), virtually all existing water resources systems have been designed on the basis of the same axiom: the past is the key to the future. We have to admit that hydrological time series contain more or less dominant non-stationary features caused by changes/oscillations in climate and large-scale quasi-periodic phenomena. The main conclusions to draw from this new insight for predictions into the future (design) is that the worth of data for such predictions has decreased (Gottschalk and Sælthun, 1990). This increase in the uncertainty can be incorporated in a risk calculation.

The influence of change in land use on hydrological phenomena is also a classical topic in hydrology starting from the studies in small drainage basins in Switzerland in the beginning of this century (Engler, 1919). Rodda (1976) gives an extensive overview. It is clear from such studies that a change in land-use, say deforestation, might have a significant influence on floods. The general conclusion from another famous study in Wagon Wheel Gap (Bates and Henry, 1928) that forest reduces the magnitude of ordinary seasonal floods and that forest maintains streamflow in dry weather is a well accepted result, which has been confirmed by many other studies for temperate climates. The critical point is how this finding can be scaled up to large drainage basins. The question of scale is central in a double respect - the scale of the change of land use and the scale of the prevailing weather phenomena. In Scandinavia drastic large scale changes in land-use are fortunately not actual. In other parts of the world the situation is different. We will return to the topic of the influence of land-use change on floods and scale for Norwegian conditions later.

Figure 6. Flooding monument with marked historical floods at Grindalen, Glomma.

3. The concept of risk

A generally used definition of risk is the Bayesian expected loss r(a) for an action a (Berger, 1985):

$$\rho(a)=\int L(\varsigma_p,a)f_Z^*(\varsigma_p)d\varsigma_p \quad (1)$$

where $L(\zeta_p,a)$ is a loss function (damage function), ζ_p state of nature (e.g. river water level or river discharge with the exceedence probability p) and $f_Z^*(\zeta)$ is the frequency function of ζ_p. In the Bayesian terminology this distribution should be the posterior distribution, updated with supplementary information in relation to a prior distribution. Berger also defines a risk function (the frequential risk), which for the present application is formulated as:

$$r(\varsigma_p,\delta)=\int_{\mathbf{x}} L(\varsigma_p,\delta(\mathbf{x}))\,f_Z(\hat{\varsigma}_p(\mathbf{x})|\varsigma_p)d\mathbf{x} \quad (2)$$

where $\delta(x)$ is a decision rule based on the vector of observations x and $f_Z(\hat{\varsigma}_p(\mathbf{x})|\varsigma_p)$ the sample distribution of the estimate of ζ_p.

The point of departure for calculation of risk of flooding is as a rule a model (regional frequency curve) for the flood discharge $f_Q(q_A)$, where A denotes the area of a drainage basin. This constitutes the prior distribution for our problem. Specifying a certain drainage basin A_i for a site i in a river, the regional model can be updated with local information at this site leading to the posterior distribution. The discharge q_{Ai} can be related to flood stage by the rating curve $q_A=g(\zeta_i)$. From the flood stage the damage (loss) L can be calculated from a stage-damage curve $l=l(\zeta_i)$. It is noted that all the three variables discharge - Q, water level - Z and damage loss - L are stochastic variables. The transformation from the peak discharge to monetary-flood loss is then given by the following equation:

$$l=l[\varsigma]=l[g^{-1}(q)] \quad (3)$$

Assume that the peak discharge Q is known to be of a particular distribution (e.g. lognormal, Gumbel, Weibull, etc.). The analytical derivation of the distribution functions for Z and L, given the random variable Q and the transformations l and g^{-1}, is straightforward (Fig. 7):

$$F_Q(q)=F_Z(g^{-1}(q))=F_L(l(g^{-1}(q)))=F_L(l) \quad (4)$$

Lambert and Li (1994) show some exact results for the derivation of the distribution function $f_L(l)$ for the damage costs from the distribution $f_Z(\zeta)$ of water stage and $f_Q(q)$ of discharge, respectively, when the family of extreme value distributions is applicable.

The risk is evaluated accordingly as:

$$r=\int_0^\infty l f_L(l)dl=\int_0^\infty l(\varsigma)f_Z(\varsigma)d\varsigma=\int_0^\infty l[g^{-1}(q)]f_Q(q)dq \quad (5)$$

It is to be noted, that the risk estimate, in this case, only reflects the uncertainty due to the inherent random characteristics of the runoff formation processes itself. Other uncertainties enumerated above in the previous paragraph are left out.

One approach to describing risk of flooding is to simply report the expected damage (loss) due to flooding. However, engineers have generally been reluctant to base decisions solely upon expected damages because the expectations can lump events causing modest damage and events resulting in extraordinary damages (Thompson 1997). Many decision-makers do not feel that such events are commensurable. A single expected value does not show trade-offs between high-cost/low probability events and low-cost/high probability events. The hydrological literature offers several alternatives. In the partitioned multiobjective risk method (PMRM) (Mitsiopolous et al. 1991) a conditioned expected damage is defined given that the damage is greater than or equal $l(p)=F_L^{-1}(p)$. Karlsson and Haimes (1988a,b) develop methodology for partitioning of probability distributions. Another alternative is the partial expected damage function i.e. the expected damage from all events greater than a threshold (Thompson et al., 1997). In the risk analysis literature risk versus damage magnitude is shown for various events (Starr 1969, Rasmussen 1981). Similarly, alternative flood control measures are often evaluated by plotting various levels of damage costs versus their exceedance probability (Parett 1987, Loucks et al. 1981, Mays and Tung, 1992). Fig. 8 illustrates the latter two alternatives.

In the approach described above the point of departure is the discharge in a river Q (a stochastic variable). In case of flooding we find it more straightforward to start from the observed critical water level ζ_c in a river, an outcome of a stochastic variable Z. With this starting point two problems are put forward illustrated by the block scheme in Fig. 9:

1. Which is the loss (damage cost) $\hat{l}=\hat{l}(\varsigma_c)$ due to the flooding caused by this high water level?
2. Which is the probability $\hat{p}=\hat{p}(\varsigma_c)$ of exceeding this water level?

To solve the first problem, i.e. establishing a stage-damage curve for a floodplain, the following factors are of major importance:

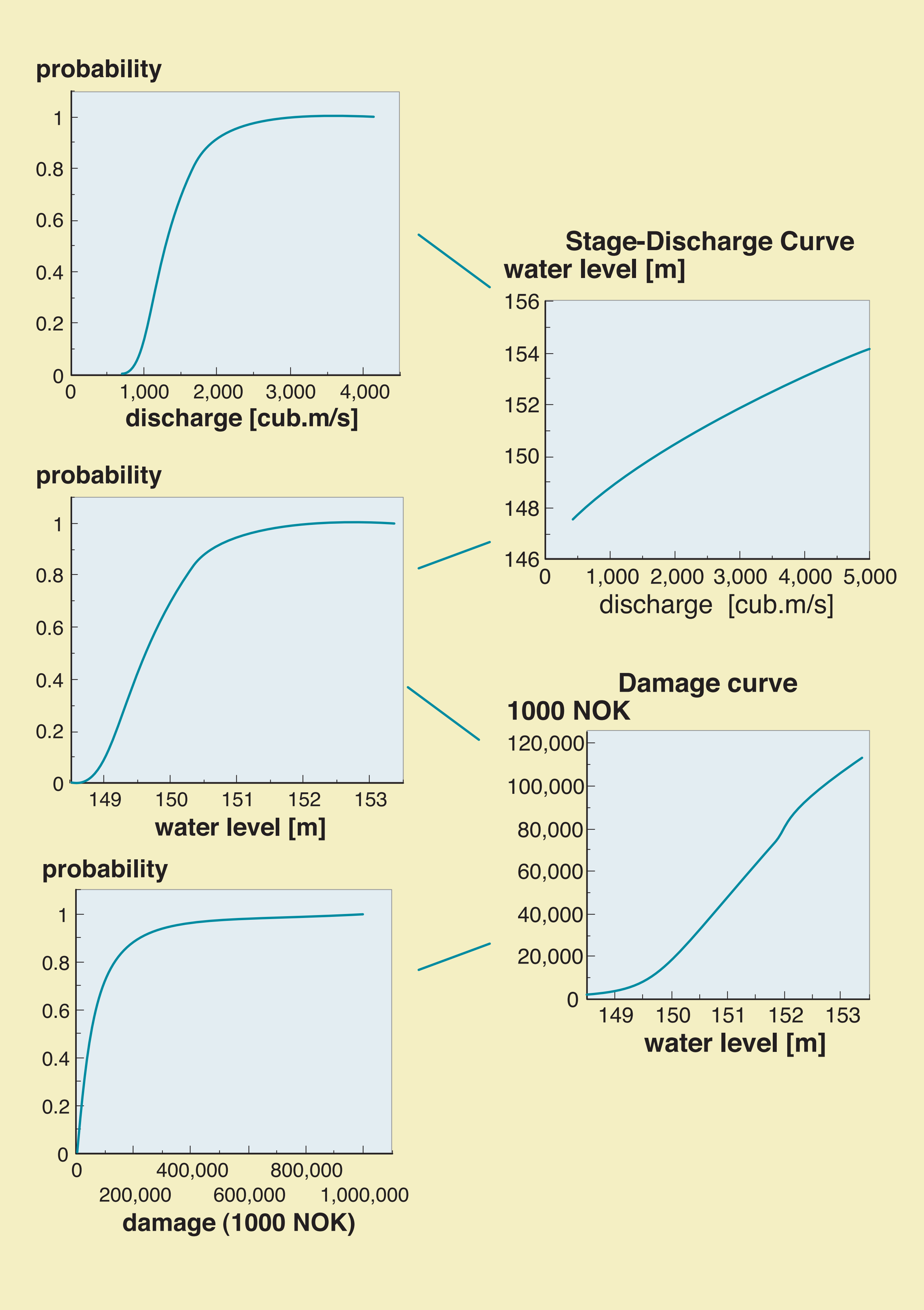

Fig. 7. Exact calculation of distribution of flood damage when underlying distribution is known (modified after Lambert and Li, 1994).

- *channel characteristics*
  - river flow profiles $\zeta_u = h(\zeta_c)$
- *floodplain characteristics*
  - economic activity (number of economic objects) N
  - topography (of objects) $F_\Xi(\xi)$
  - levels of dikes etc. ξ_0
  - economic loss (as a function of local water level η) $F_C(c|\eta)$
- *uncertainties*
  - accuracy in topographic data
  - accuracy in economic loss estimates
  - accuracy in estimated flood profiles

For the second problem factors of importance are:

- Exceedance probabilities of floods
  - magnitude of floods in main river $F_Q(q_A)$
  - magnitude of floods in headwaters $F_Q(q_{ai})$
  - synchronicity of floods in headwaters $\rho(q_A, q_{ai})$
  - effects of river regulation
- channel characteristics
  - stage discharge relation at downstream critical section $q_A = g(\zeta_c)$
- uncertainties
  - accuracy in estimation of exceedance probabilities of floods
  - accuracy in stage discharge relation

Herein an approach for solving these two problems is presented based on the factors listed above.

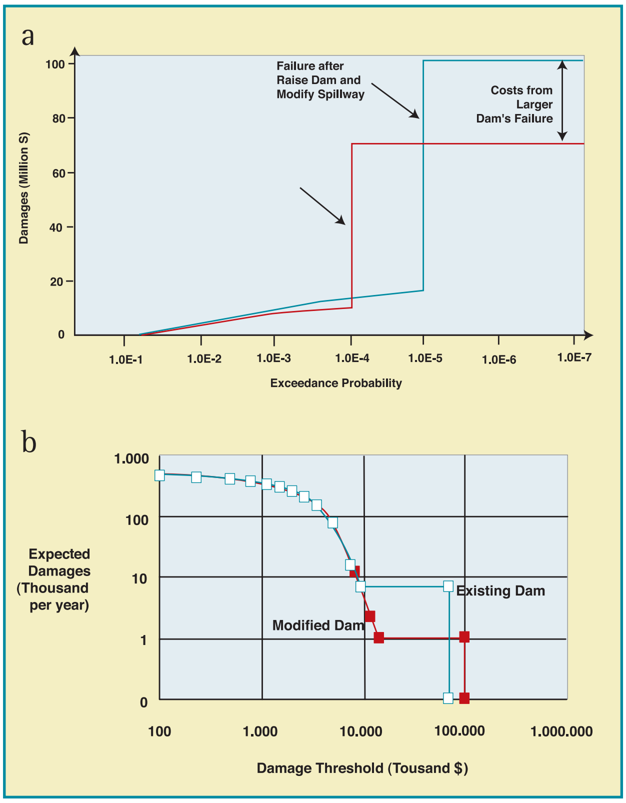

Fig. 8. Distribution of damages from major floods (a) and the partial expected damage function (b) illustrating effect of raising dam and widening spillway (from Thompson et al., 1997).

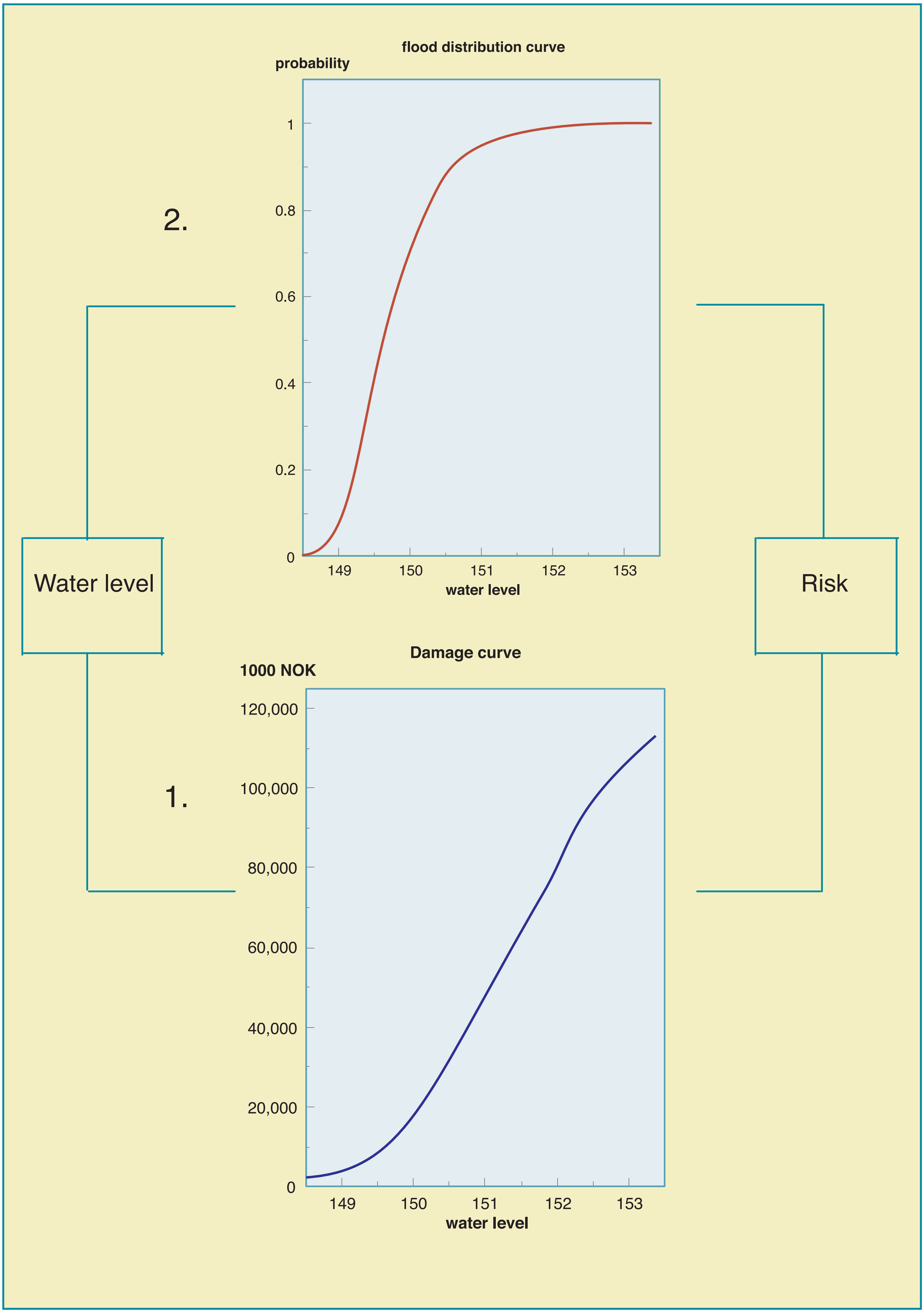

Figure 9. A block scheme illustrating the basis for risk calculation herein.

4. The Stage-Damage Curve

The resistance to flooding is directly connected to the topographic position of objects (buildings etc) that could be damaged by the floodwater. Each individual object i is identified by its absolute altitude ξ_i. The distribution of the altitudes (ground floor level of the building) of about 3870 buildings in Grue and Åsnes municipalities along 32 km long section of the Glomma River has been analysed (Fig 2). For the further analysis the river section along the floodplain (26 km in south-north direction) was partitioned into 18 clusters of settlements. Eight of these clusters are protected against flooding by a system of dikes designed to withstand a flood of the magnitude of the one in 1916. The histograms of topography of objects are illustrated in Fig. 10. It can be noted that the northernmost clusters (no 8 and 9) show as low altitudes as those do in the south. The natural slope of the river along the section is about 0.08 permille at natural water stages and 0.14 permille at high floods (the 1995 flood) which then means a difference in water level of 2.07 m and 3.52 m, respectively, between the downstream and upstream limits.

In the following the distribution of the sample (Cramér, 1971) of altitude of buildings:

$$F_{\Xi}^*(\xi) = n/N \tag{6}$$

, where n denotes the number of sample values ξ_i that are $\leq\xi$ of totally N values, will be directly used to represent the cumulative distribution of altitude of buildings $F_{\Xi}(\xi)$.

4.1 Consequence value determination

A local critical water level for flooding is defined as the depth $\eta_i=\zeta-\xi_i$. As long as the water level ζ in the river is low, η_i is negative. When this level is higher than the ground floor of the building, η_i is positive. The exact value of η_i resulting in flooding of an object varies with the type of the construction of a building and the local topography. The damage brought about by the floodwater is rather to see as a function of η_i, the higher the level η_i the higher the damage. Over some critical level of η_i the damage is total and does not increase further.

The flooding of houses is the main reason for loss (damage) due to extremely high river water levels in a surrounding floodplain with an urban settlement. The value loss for an individual house is related to the height of the local water level η (Fig. 11). There is a considerable scatter in the data but the dependence on the height η is obvious. It is notable that the increase of the costs starts already at negative values of η (i.e. increase in the floodplain groundwater level). An increase of the groundwater level will of course have an effect on the likelihood of moisture damages, especially if the house has a cellar. The figures in Fig. 11 are real costs as paid by insurance companies for flood damage after the 1995 flood. From the literature review in Ch. 2 of this report we learned that other factors than the depth of water influence the severity of damage. This may be so but these differences do not show up in the damages estimated by insurance agents.

The relation in Fig 11 is not reasonably well approximated by a deterministic function; the scatter is too big. Instead a distribution function conditioned on the height η is suggested. The cost for damage L′, for an individual house, is in this case looked upon as a stochastic variable with the pdf $f_L'(l'|\eta)$. For low values of η (negative) the probability for relatively low costs (with a modal value at zero) is dominating indicating a J-shaped distribution. For increasing values of η the centre of gravity of the costs moves away from the zero axis, giving rise to a clock formed distribution. The distribution is asymmetrical with a tail towards high costs (positive coefficient of skewness). Here due to the large scatter and for simplicity the cost is taken as expected values E[l′] and standard deviation D[l′] for classes of the local water level. Only two classes have been used in the further calculation:

- $-2.5<\eta\leq-0.5$; E[l′]=48.1 kNOR; D[l′] =41.7 kNOR (low damage) (7)
- $-0.5<\eta$; E[l′]=411.9 kNOR; D[l′] =293.9 kNOR (high damage)

It is open for a more detailed analysis at a later stage.

4.2 Number of flooded objects

When all objects on a floodplain are considered, the levels η_i;i=1,..,N, where N is the total number of objects (buildings), can be looked upon as a random variable H dependent on the river stage ζ. It is characterised by its conditional cdf (pdf) $F_H(\eta|\zeta)$ ($f_H(\eta|\zeta)$). It is further necessary to consider that the water level in the river varies along a river section. The analysis of the data on the altitude of buildings shows that there is no dependence between this altitude and the south-north direction (the main direction of the river). We can thus assume that the water level in the river and the altitude of buildings are independent. For a river section the water level in the river can thus be represented by a rectangular distribution:

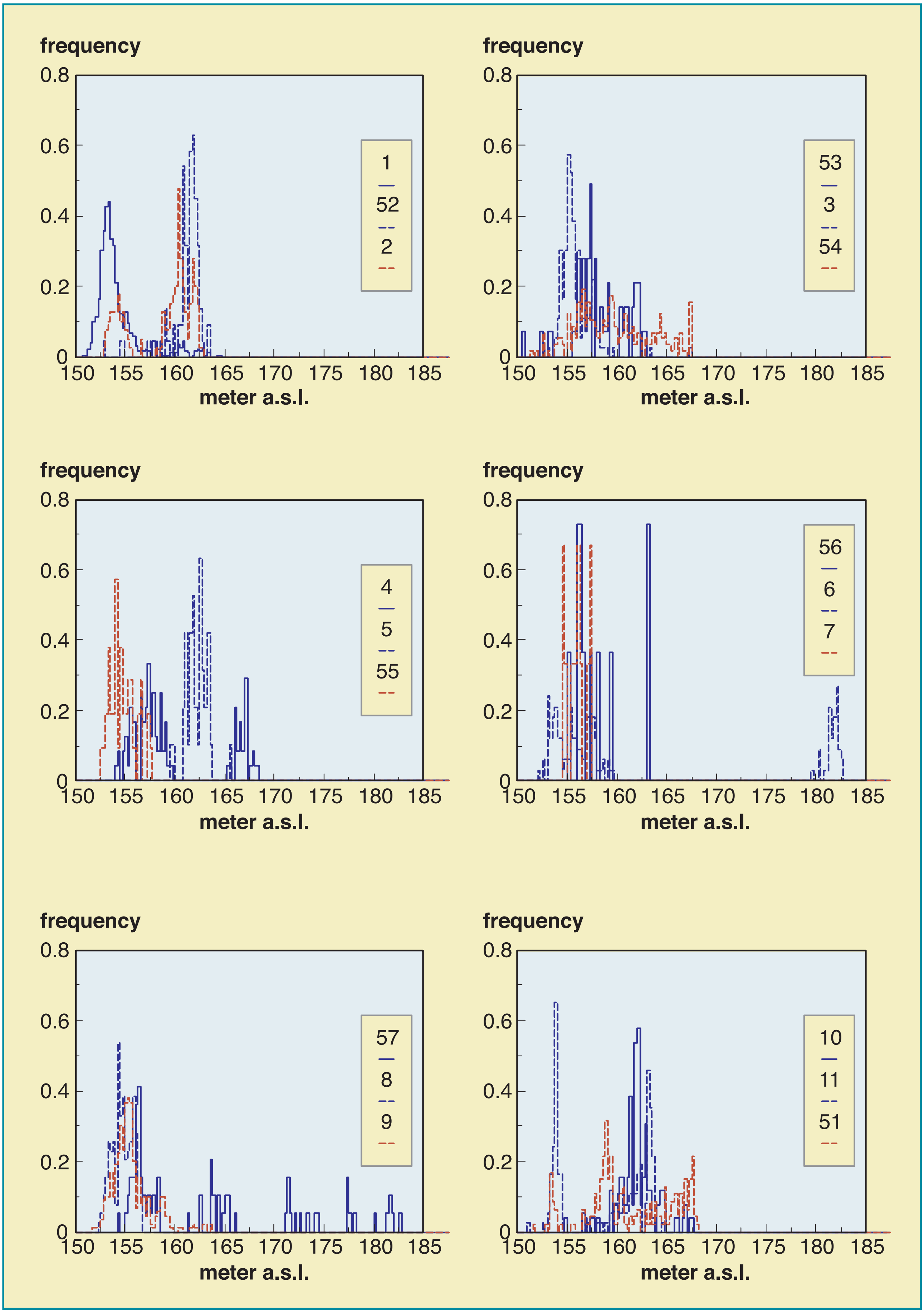

Figure 10. Frequency histograms $f_{\Xi}(\xi)$ for the altitude of buildings ξ for flood plain clusters along the Glomma River.

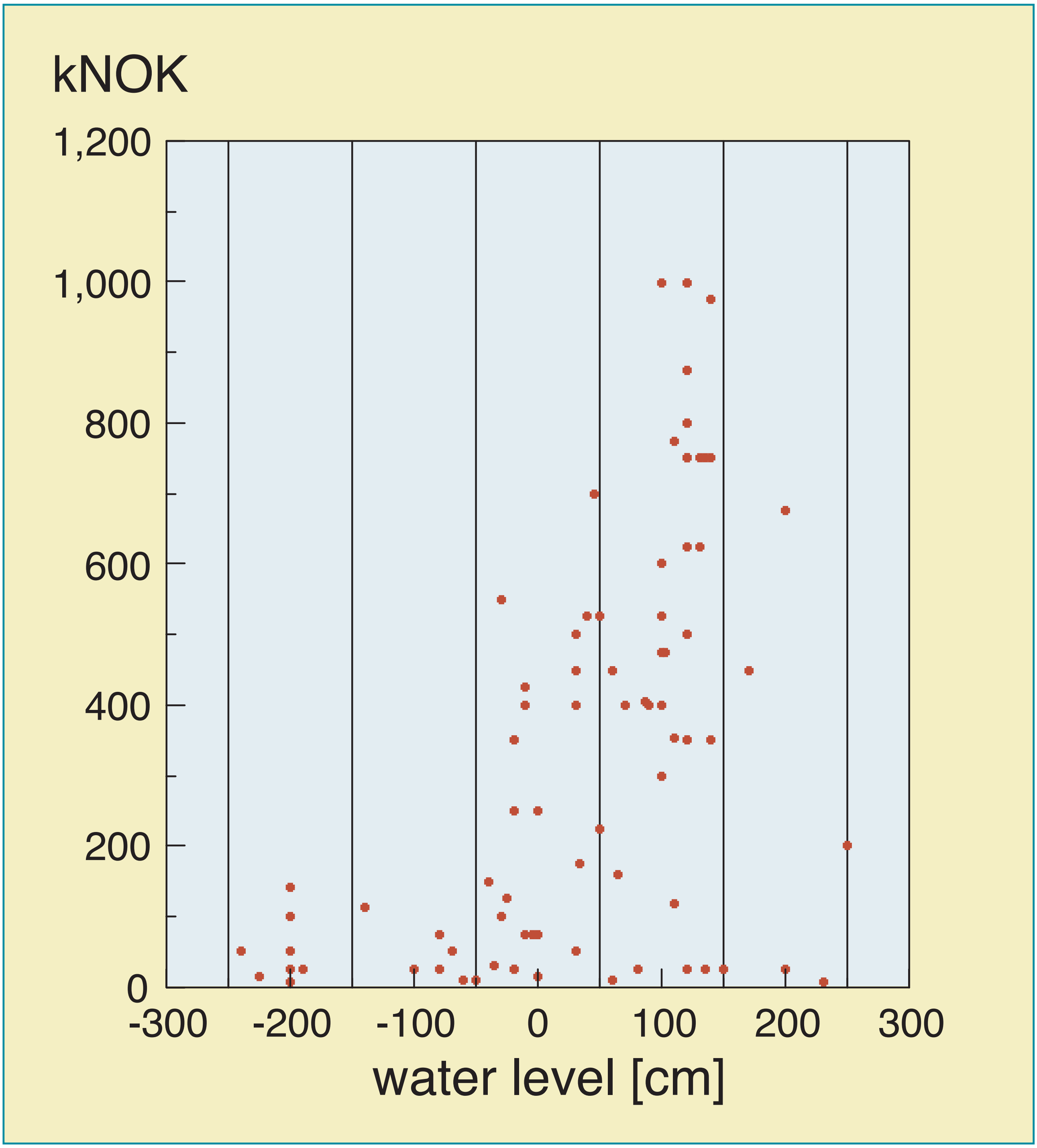

Figure 11. Relation between local water level η and individual cost of damage l' (from M. Wathne,1998).

$$f_Z(\zeta) = \frac{1}{\zeta_u - \zeta_d} \tag{8}$$

where ζ_u and ζ_d are the water levels at the upstream and downstream points, respectively, of the river section. The water levels in the river are all established in relation to the gauging station at Nor (see Fig.12). The following relation has been developed for calculating the water level ζ_L at a distance L meters upstream Nor:

$$\zeta_L = \zeta_{Nor} + L(1.082\zeta_{Nor} - 151.78)\,10^{-5} \tag{9}$$

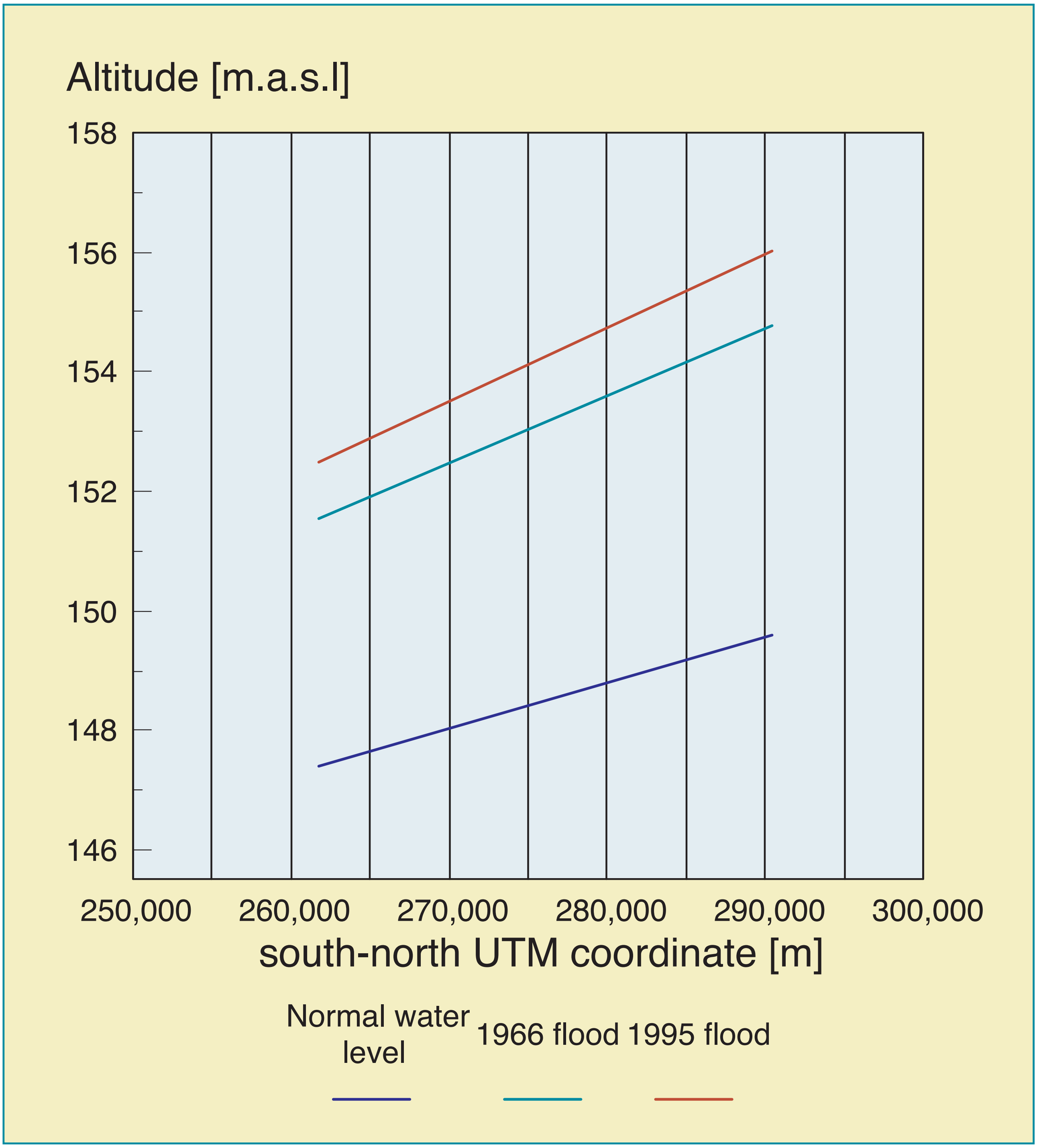

Figure 12. Profile of the Glomma upstream the gauging station at Nor.

The water level in a building $\eta=\zeta-\xi$ is determined as the difference between two random variables ζ and ξ. Utilising well known relations from probability theory (see for instance Springer, 1979) the frequency distribution of h is formally derived as:

$$f_H(\eta|\zeta_u,\zeta_d)=\frac{1}{\zeta_u-\zeta_d}[F_\Xi(\zeta_u-\eta)]; \qquad \zeta_d-\xi_0\leq\eta<\zeta_u-\xi_0$$
$$f_H(\eta|\zeta_u,\zeta_d)=\frac{1}{\zeta_u-\zeta_d}[F_\Xi(\zeta_u-\eta)-F_\Xi(\zeta_d-\eta)];\ \eta<\zeta_d-\xi_0 \qquad (10)$$

where ξ_0 is the lower bound of the distribution of altitude of buildings. It thus follows that the derived distribution has an upper bound equal to $\eta_{max}=\zeta_u-\xi_0$, the largest water depth in an individual building. It is also to be noted that in case the distance between the upstream and downstream points is small the distribution eq. (10) has the limiting form:

$$f_H(\eta|\zeta_u,\zeta_d)=\frac{1}{\zeta_u-\zeta_d}[F_\Xi(\zeta_u-\eta)-F_\Xi(\zeta_d-\eta)]\longrightarrow f_\Xi(\zeta-\eta)$$
$$for\quad \zeta_u\longrightarrow\zeta_d=\zeta \qquad (11)$$

In the following the relation eq. (9) will be utilised and all water depths in buildings will be related to the river stage at Nor ζ_{Nor} and the distribution eq. (10) expressed as $F(\eta|\zeta_{Nor})$. The latter distribution has been calculated for two cases, which are illustrated in Fig. 14, namely for the floods in 1966 and 1995 with water levels at Nor equal to ζ_{Nor}=151.53 m and 152.49 m, respectively. Only water depths $\eta>0$ have been considered in the upper graphs, while the lower graphs show the full conditional distributions. The latter curves indicate that for the main part of the buildings the water levels are well below the ground floor (η negative). For comparison the corresponding distributions for positive values of η derived from a terrain model in a GIS framework (Astrid Voksö, personal communication) are given. The agreement is very good which supports the applied statistical approach for deriving these distributions.

For a fixed critical value of η_c the number of buildings n (of totally N) with a local water level $H>\eta_c$ is evaluated from:

$$n(\eta_c|\zeta_{Nor})=N\int_{\eta_c}^{\eta_{max}}f_H(\eta|\zeta)d\eta \qquad (12)$$

,

and the number of houses Δn within an interval $\Delta\eta$ around $(\eta_c|\zeta_{Nor})$ is:

$$\Delta n(\eta_c|\zeta_{Nor})=Nf_H(\eta_c|\zeta_{Nor})\Delta\eta \qquad (13).$$

It is these latter measures of the number of buildings with a certain critical local water level that will be useful when estimating the risk of flooding. Fig. 14 illustrates how these functions of ζ_{Nor} for the critical intervals for damage eq. (7) (low: $-2.0<\eta<-0.5$, high: >-0.5) look like for the present set of data (full lines). The number of buildings with low damage (red curve) first increases to reach a maximum and then decreases as more and more buildings turn into the class of high damage (Fig. 14a). The number of buildings with high damage (blue curve) is monotonously increasing but with a slow rise for low water levels. The curve for total damage (green line) is the sum of the two other curves and it is also monotonously increasing. Fig. 14b shows the same three curves but with consideration of the dikes. The principal differences between the three curves are the same as in Fig. 14a but the effect of the dikes is dominating the picture with a very sharp increase in the number of damaged buildings at water levels at Nor between 151.75 and 152.00 m.

4.3 Effect of uncertainty in topography

The topographic data of buildings is evaluated from maps with a contour interval of 1 meter. Maps with contour intervals of 5 and 10 meters have also been used to test the influence of the precision in the map information. The precision in map data σ_M can be estimated to 30% of the contour interval (Watt and Paine, 1992). To be able to evaluate the influence of the precision in the estimation of number of flooded buildings the empirical distribution eq. (6) is replaced by (it is assumed that the errors in map data follow the normal distribution):

$$F_\Xi(\xi)=\frac{1}{N}\sum_{i=1}^{N}\Phi\left(\frac{\xi-\xi_i}{\sigma_M}\right) \qquad (14),$$

where $\Phi()$ is the cdf of the normal distribution. The results of applying eq. (12) to calculate the number of damaged building are also shown in Fig. 14. The general effect is a smoothening of the curves in respect to the empirical data. The 1-m contour interval curves follow well those of the empirical data while for map data from maps with 5 and 10 m contour interval almost all details have been wiped out. It is to be noted that it is assumed that the precision in the data of the topography of the dikes is only 10 % of the contour interval. That is why the effect of the dikes in Fig. 14d is rather distinctly reproduced for all three cases.

The effect of errors has been brought one step further. The expected number of erroneously classified objects has been calculated (Table 2). Two types of errors occur. The first one is when an object really belongs to say the class of buildings with high damage but is classified as not being in this class (type 1 error). The second one is when an object not really belonging to the class is classified as being in the class (type 2 error). In relative terms these errors are biggest when the number of objects is low. The type 1 error is then related to the number of objects classified while the type 2 error is related to the number of objects in the rest of the sample. In round figures the errors are 10-15 % for maps with 1-m contour interval, 20-30 % for 5 m and 40-50 % for 10 m.

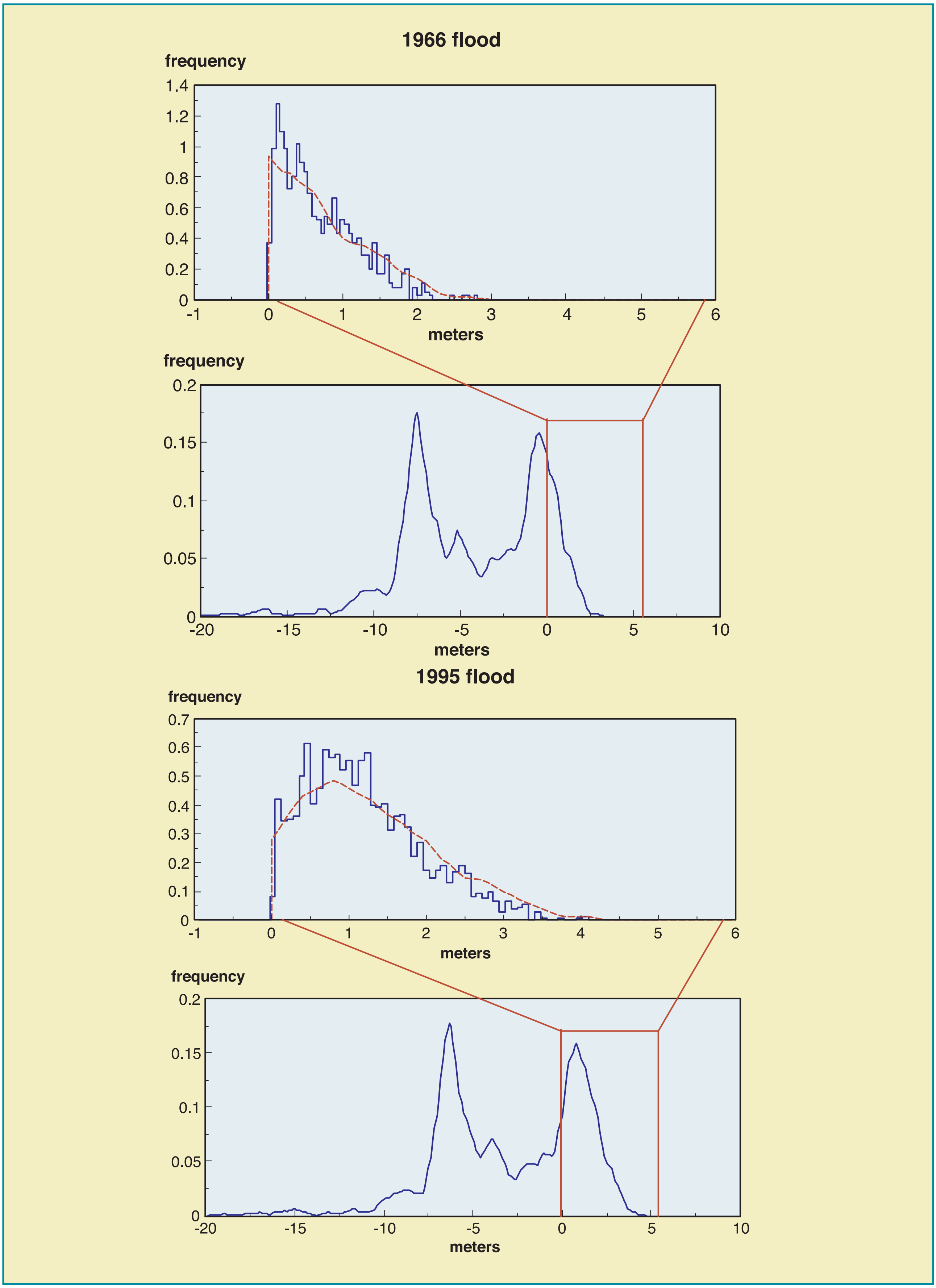

Figure 13. Conditional distribution $f_H(\eta|\zeta_{Nor})$ of the critical local water level η for the 1966 year flood ζ_{Nor}=151.53 and the 1995 year flood ζ_{Nor}=152.49. Upper graphs show the distributions for η>0. The full line represents curves derived from GIS calculations, while the dotted line shows curves derived from eq. (10). The lower graphs show the distribution for all η.

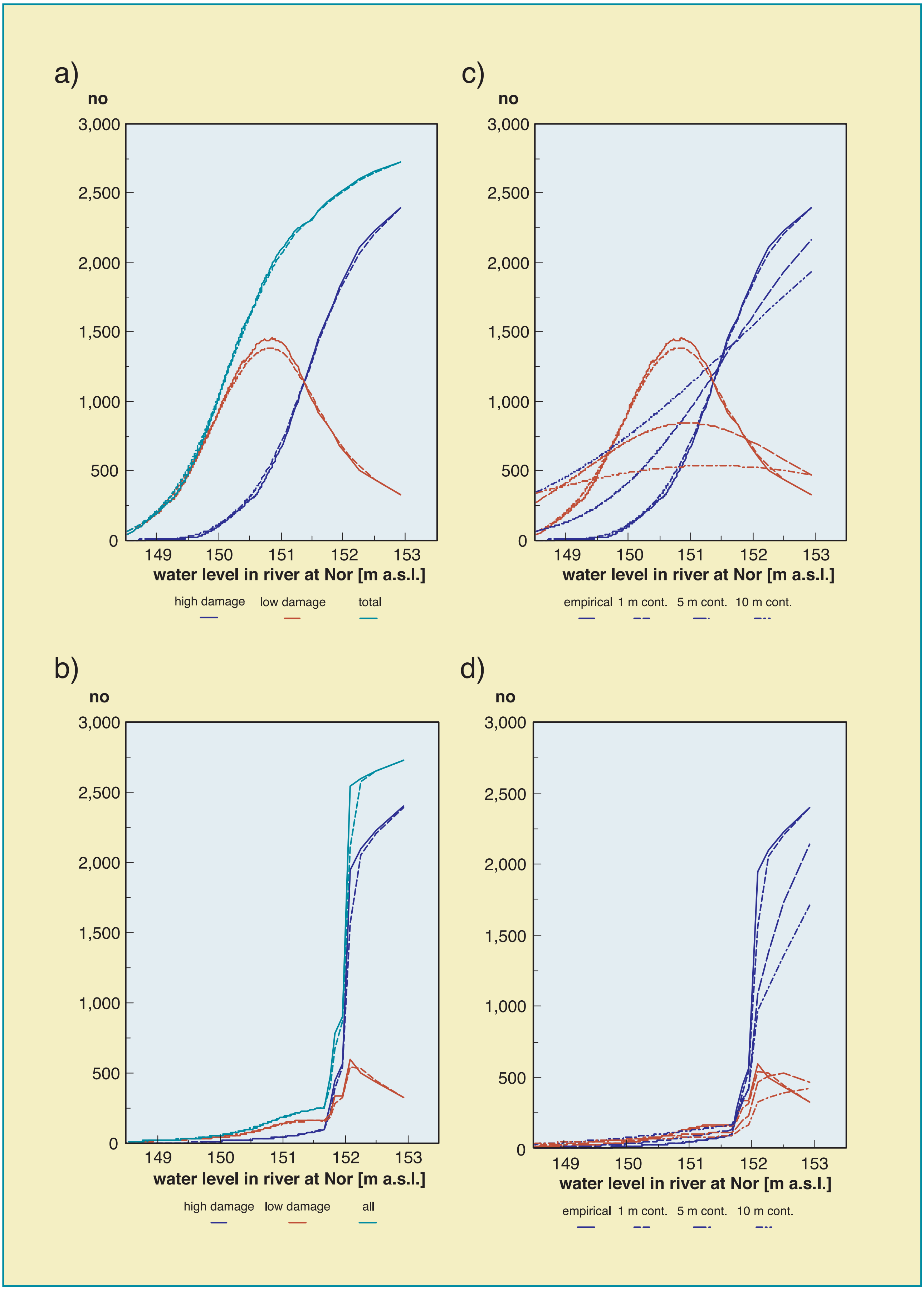

Figure 14. The number of objects flooded $n(\eta|\zeta_{Nor})$ with low (red line) and high damage (blue line) and the sum of the two (green line) as a function of the river water stage ζ_{Nor} . In a) and c) existing dikes are neglected and in b) and d) their role is taken into consideration. c) and d) illustrates the role of precision in the map data.

Table 2. Expected number of misclassified objects for different precision in map information.

water level ζ_{Nor} at Nor	number of objects	type 1 error			type 2 error		
		map contour interval					
		1 m	5 m	10 m	1 m	5 m	10 m
high damage, no dikes							
149.0	4	0.5	1.35	1.7	1.7	133.1	462.5
149.5	15	2.7	5.7	6.5	11.4	234.8	586.2
150.0	114	26.1	47.3	51.9	36.3	362.9	702.1
150.5	302	39.9	111.1	130.0	70.1	479.3	771.8
151.1	852	111.5	293.5	354.5	130.6	488.0	691.7
low damage, no dikes							
149.0	199	33.1	79.4	89.2	54.2	349.7	558.1
149.5	470	72.0	175.3	204.0	106.6	398.2	352.5
150.0	971	131.7	354.0	416.1	151.1	364.9	702.1
150.5	1354	109.6	446.2	555.8	139.1	314.2	252.5
151.1	1333	69.0	390.2	519.5	153.2	345.8	274.0
high damage, with dikes							
149.0	2	0.2	0.7	0.9	0.3	9.3	42.1
149.5	4	0.5	1.3	1.6	1.7	16.1	55.5
150.0	15	1.9	5.4	6.4	2.6	23.9	69.4
150.5	28	2.6	8.8	11.1	3.1	35.4	84.1
151.1	54	5.1	15.3	20.3	6.4	53.4	100.9
low damage, with dikes							
149.0	18	2.1	6.6	7.8	2.5	24.2	40.6
149.5	30	3.5	10.1	12.4	3.6	34.4	46.8
150.0	43	5.1	15.0	18.1	10.6	49.1	53.8
150.5	77	9.8	27.7	32.8	19.3	55.5	55.7
151.1	152	13.8	51.9	63.4	15.8	46.9	50.5

4.4 Stage-damage curve for the flood plain at Nor

The number n, of totally N, of buildings that will be damaged by flooding on a floodplain increases with increasing level ζ of the river as shown by eqs. 12 and 13, and Fig. 14. The expected number of buildings with local water level $\geq\eta_c$ when the river stage is ζ is $\Delta n(\eta|\zeta_{Nor})$ (eq. 12). The expected damage cost for individual buildings is $l'(\eta)$ (eq. 7), and the expected total cost $l(\eta,\zeta)$ is thus:

$$l(\eta,\zeta)=\Delta n(\eta|\zeta)\,l'(\eta) \tag{15}$$

The distribution function of $l(\eta,\zeta)$ is evaluated from (15) as:

$$f_L(l|\eta,\zeta)=f_{L'}(l(\eta,\zeta)/\Delta n(\eta,\zeta))/\Delta n(\eta,\zeta) \tag{16}$$

The expected damage $E[L|\zeta]$ for a certain interval of critical damage say $\eta>\eta_c$ is derived by integration over the critical interval:

$$E[L|\zeta]=\int^{\eta_{max}} l\, f_{L'}(l(\eta,\zeta)/\Delta n(\eta,\zeta))/\Delta n(\eta,\zeta)\,d\eta \tag{17}$$

For the present case when the distribution of individual damage cost is simplified into only two values for high and low damage, respectively, (eq. 7) the expected damage can be evaluated from:

$$E[L|\zeta]=\begin{cases} n(-2<\eta\leq -0.5|\zeta)l'_{low} \\ n(\eta>-0.5|\zeta)l'_{high} \end{cases} \quad (18)$$

This function - the stage-damage-curve- a function of the water stage ζ_{Nor} at Nor is shown in Fig. 16 for low and high damage and the sum of the two - the total damage (1-m contour interval data). It is mainly a reflection of the number of damage buildings shown in Fig. 14. The expected errors in the number of damaged buildings (Table 2) are of course also relevant for the stage-damage-curve. A further source of uncertainty is added as revealed by the standard error in the estimates of damage costs for individual buildings (eq. 7). Table 3 illustrates the order of magnitude of this error in terms of its standard deviation D[L]. This error is thus large when only a few objects are concerned but its relative importance is significantly reduced as the number of damaged buildings increases.

Table 3. Errors in loss estimates due to variability of damage costs of individual buildings.

water level ζ_{Nor} at Nor	number of objects	$E[L\|\zeta]$ kNOK	$D[L\|\zeta]$ kNOK	$D[L\|\zeta]/E[L\|\zeta]$
		high damage, no dikes		
149.0	4	1648	588	0.356
149.5	15	6179	1138	0.184
150.0	114	46957	3138	0.067
150.5	302	124394	5107	0.041
151.1	852	350939	8579	0.024
		low damage, no dikes		
149.0	199	9572	588	0.061
149.5	470	22607	904	0.040
150.0	971	46705	1299	0.029
150.5	1354	65127	1534	0.024
151.1	1333	64117	1756	0.027
		total damage, with dikes		
149.0	203	11220	832	0.074
149.5	485	28786	1454	0.050
150.0	1085	93662	3396	0.036
150.5	1656	189521	5333	0.028
151.1	2185	415056	8757	0.021

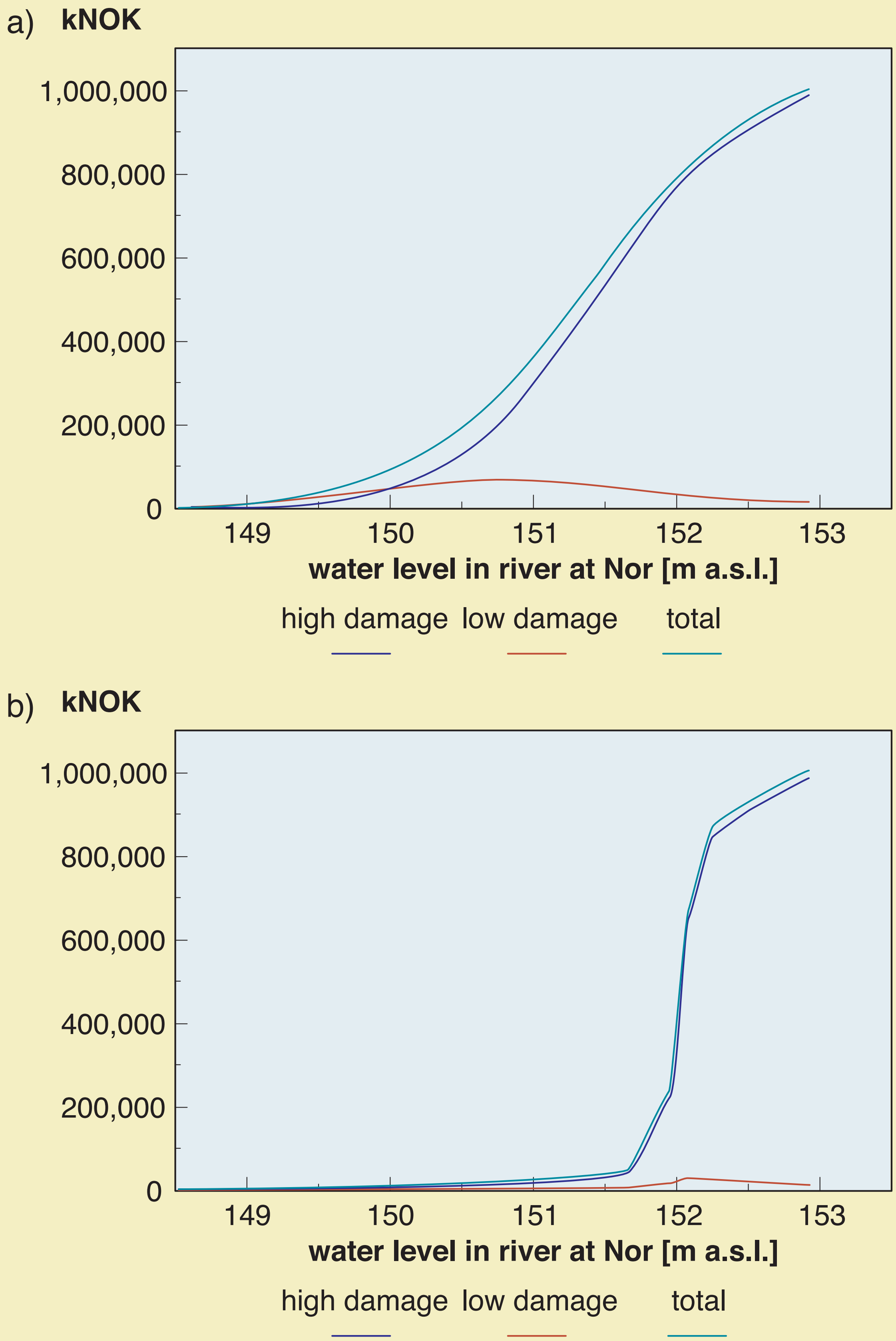

Figure 15. Stage-damage-curve for the floodplain upstream Nor based on 1-m contour interval map data.

5. Flood Stage Exceedance Probability

The probability of exceeding a critical water level in the main river is:

$$P(Z > \zeta) = 1 - P(Z \le \zeta) = 1 - F_Z(\zeta) \qquad (19)$$

This water level corresponds to a certain discharge q in the river determined by the stage-discharge relation g( ) for the river site:

$$q = g(\zeta) \quad or \quad \zeta = g^{-1}(q) \qquad (20)$$

There are three different stage-discharge curves established at Nor (Fig. 16). In the lower register the curves coincide well, which is not the case for higher discharges. It is assumed that the latest established curve (1975-) is the most reliable and it is used here for all years before and after 1975. The standard error in the discharge calculated from river stage is estimated to 72.7 m^3/s applying ordinary logarithmic regression. The probability of exceedance of corresponding values of q and of z are of course identical, i.e.:

$$P(Z > \zeta) = P(Q > q), \text{ equivalent to } F_Z(\zeta) = F_Q(q) \qquad (21)$$

The relation between the corresponding pdfs is:

$$f_Z(\zeta) = f_Q\left(g^{-1}(q)\right)\frac{dg^{-1}(q)}{d\zeta} \qquad (22)$$

5.1 A regional frequency curve for floods in Glomma

Floods and their distribution function $F_Q(q)$ are in Norway determined by so called regional growth curves (cdfs) (Tveito, 1993). The construction of these regional flood frequency curves is based on the index flood approach (Dalrymple, 1960). It consists of two parts. The first part is the development of a basic dimensionless frequency curve representing the ratio of the flood of any frequency to an index flood (e.g. the mean annual flood). The second part in the index flood approach is the development of relations between drainage basin characteristics and the index flood (the mean annual flood), to allow prediction of the mean annual flood at any point within the region. Recently the main emphasis has been on the development of statistically robust regional estimators of flood distributions, so called L-moments (Hosking 1990, Vogel and Fennessey, 1993), the identification of distributions and the delineation of homogeneous regions in which the index flood assumption holds. Hosking and Wallis (1993) have suggested methods to test this assumption.

During the last few years a new theoretical framework has evolved which is aimed at understanding the stochastic structure of regional floods in terms of their physical generating mechanisms. This framework for regional flood frequency is based on contemporary ideas of scaling invariance (Gupta et al. 1994, Smith 1992). One of the key issues is to understand how the scaling invariance in floods is related to that in precipitation (both rainfall and snowmelt) and to the three dimensional geometry of river networks (Gupta and Wymire 1996, Gupta and Dawdy 1994, 1995). Regional flood frequency approaches are mostly based on the index flood assumption which in the new scaling terminology is equivalent to an assumption of so called simple scaling. Studies of empirical frequencies of river runoff from the 1960's (e.g. Dawdy, 1961, Francou and Rodier, 1967), gave evidence which can be interpreted as showing departure from simple scaling in log-log plots of empirical moments of river flows versus spatial scale. This behaviour is termed multiscaling. Current analysis of extensive data sets demonstrates that the index flood assumption (simple scaling assumption) does not hold widely (Gupta et al. 1994, Gupta and Dawdy 1994, Blöschl 1996).
Here an approach to construct a regional flood frequency curve by Gottschalk and Weingartner (1998) is applied based on scaling relations of regional floods in terms of L-moment and expected order statistics. The L-moments are weighted linear sums of expected order statistics. A scaling relation is introduced for the expected order statistics, which allows the derivation of scale dependence of L-moments and L-moment ratios. These are used to derive expressions for the scale dependence of the parameters of the General Extreme Value (GEV) distribution with the Gumbel (Extreme Value type 1, EV1) as a special case. Three different data sets have been prepared from 35 daily observation records of at least 15 years from the Glomma drainage basin (Fig. 3), namely annual maximum series (AMS), partial duration series (PDS) (on the average 3 events per year) and synoptic partial duration series (SPDS). In the latter synoptic data set, the events at the most downstream station have guided the selection of upstream events contributing to the flood downstream within a time lag of up to 8 days. The data cover a range in drainage areas from 40 km^2 to 40000 km^2.

The scale dependence of the three parameters u, a and k of the GEV distribution is shown in Fig. 17 where the individually determined parameters are compared with theoretically calculated ones with the scaling model for PD-series. For the first two parameters the dependence is obviously very strong. For the parameter k, which is the parameter determining the type of basic extreme value distribution, the dependence is less obvious. k is

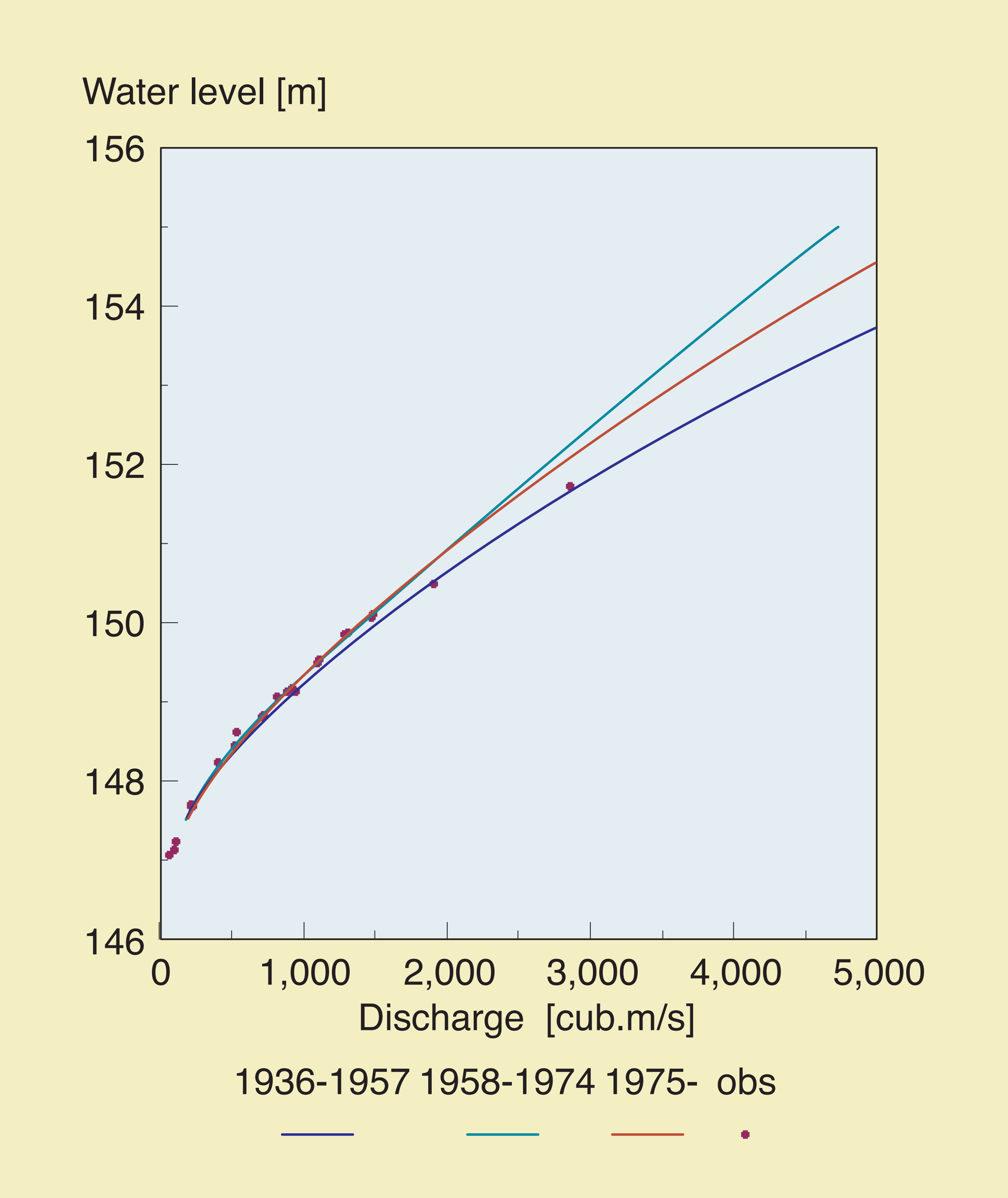

Figure 16. Stage-discharge curves at Nor.

anyhow always negative which indicate a Frechét type of distribution. Table 4 shows the standard errors in the estimates of parameters by the regional scaling model.

The derived regional frequency curve for the second data set (PDS) is illustrated in Fig. 18. The AMS have also been used to construct this regional curve with only slight differences compared to the PDS. The latter is based on more events and that is why it is considered to be more reliable. The maximum flood for different probabilities of exceedance and for different scale (area in km^2 divided by 100) is expressed as normalised values with respect to the index flood (the mean flood). The normalised flood is strongly dependent on the scale especially for small probabilities of exceedance. The size of the drainage basin has a dampening effect on the relative magnitude of the flood. A 1/100 year flood can be expected to be 2 times as big as the index flood when the basin is 50000 km^2, but almost 3 times as big for a basin of 10 km^2. For the 1/1000-year flood the corresponding values, with which the index flood should be multiplied, are 3 and 5, respectively.

5.2 Exceedence probabilities for recent flood events

Empirical data from three events from the SPDS data set are included in the graph namely the floods 1966, 1967 and 1995. It is seen that the observation points in the main branch of the Glomma and the Laagen are well kept together, indicating that the 1966 and 1967 floods had probabilities of exceedance of the order of 1/50 in the Glomma, while it was somewhat higher in the Laagen. The 1995 flood had a probability of exceedance of a little lower than 1/100 years in the Glomma and around 1/100 in the Laagen. The observed floods for the largest area (40221 km^2) indicate higher probabilities of exceedance. The large lake Mjøsa just upstream this gauging station has a dampening effect similar to that of scaling, which is not taken into consideration. The lake is usually at its lowest when the snowmelt flood starts. For pure rain-induced floods the influence can be different. The probability of exceedance (and the return period) is a well-established concept in hydrology and widely in use. It must be remembered that there is a large uncertainty connected to estimates of the probability of exceedance (see 4.4 below). Hopefully, the regional flood frequency curve for floods the Glomma shown here gives a consistent tool for estimating such probabilities of exceedance for the whole basin and minimising the uncertainties. The scatter of the points is still considerable which reflects the statistical errors. Erichsen (1995) has evaluated the return period of the 1995 flood. He used a more traditional approach and fitted one or more distribution function (of a selection of 5 theoretical distributions) to data from the Glomma drainage basin. The result was that the flood in 1995 was a rare flood in the central parts of Gudbrandsdalen and Østerdalen with a return period of about 200 years. On the west side of Gudbrandsdalen the estimated return period is 5 to 10 years. For the main Glomma River the corresponding interval for the return period is given as 100 to 200 years. When the flood reaches the Øyeren Lake the flood is dampened and the estimated return period is 50-100 years. Erichsen in his report also underlines the large uncertainties involved in the estimation of return periods.

Having stressed the large uncertainties involved in estimating probabilities of exceedance for floods in a basin, it is also necessary to note that the fact that a 1/100 flood is observed in a downstream part of a basin does not imply that the floods upstream have this very same probability of exceedance. It is rather on the contrary. From the scatter of points in Fig. 18 we see that the floods in the headwaters have very different but usually high probabilities of exceedance. How can then these relatively small common floods create the rare flood downstream?

Table 4. Standard errors in the estimation of scale dependent regional parameters of the GEV distribution.

Series	σ_u	σ_α	σ_k
AMS	166.8	21.2	0.043
PDS	121.1	29.4	0.053

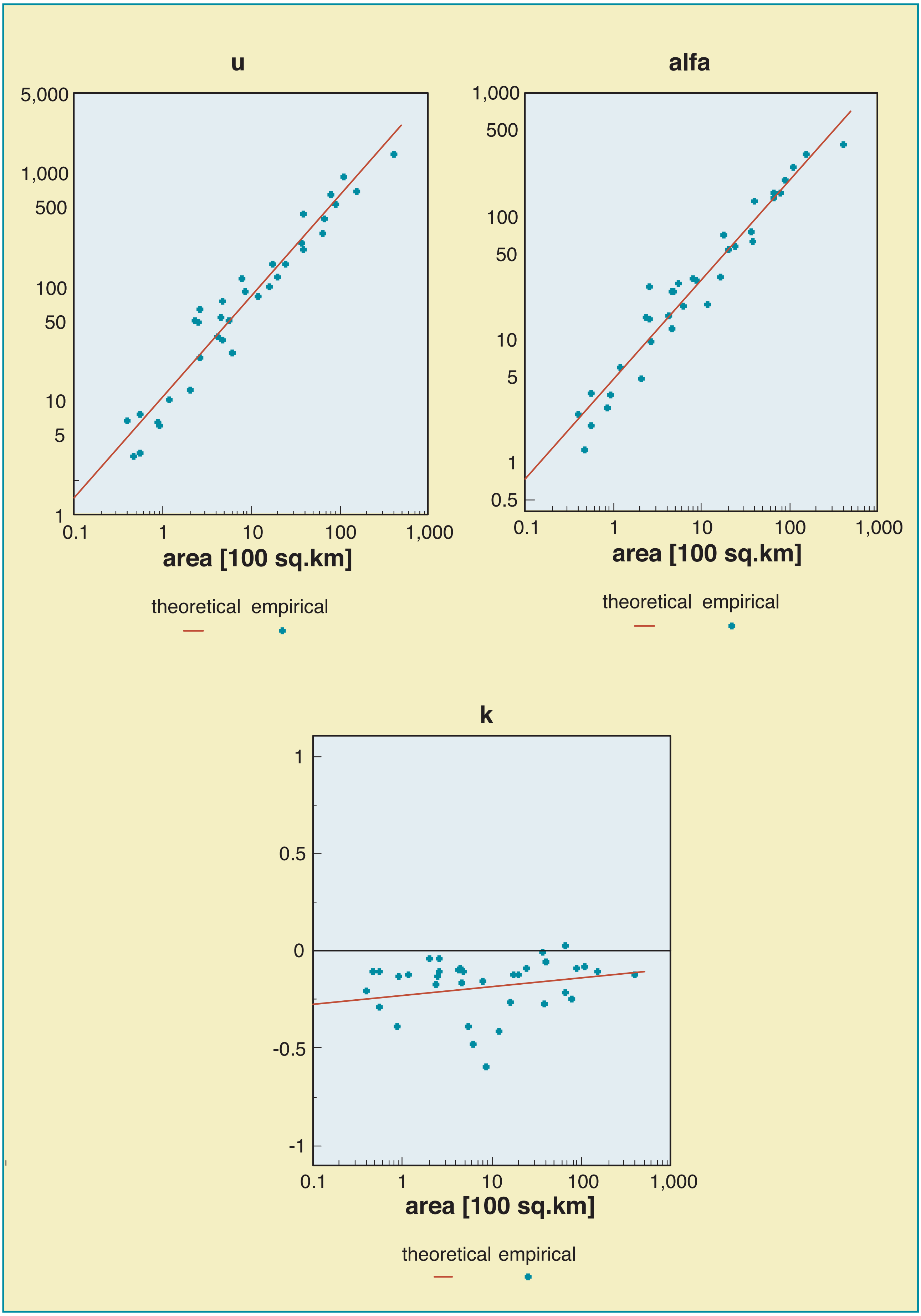

Figure 17. The scale dependence of the three parameters u, a and k of the GEV distribution for the Glomma drainage basin.

The focus in the debate around the frequent flooding in Europe during the last years has been on the influence of changes in land use on the magnitude of floods in headwaters, which in its turn should have caused an increasing risk of flooding downstream. This aspect has been the main problem behind the initiation of the HYDRA project. A major conclusion from the present analysis is that the individual magnitude of floods in headwaters is a factor of a second order to explain downstream flooding. It is hardly worthwhile to analyse observed series from downstream reaches in a hope to detect effects of land-use changes in headwaters. The eventual changes will totally drown in the variability in the magnitude of floods caused by the primary factor behind downstream extreme floods, namely the synchronicity in time of flood events in headwaters. A flood with, say, a 1/5 probability of exceedance in a headwater is likely to happen every year somewhere in a drainage basin. However, it is rarely that the flood is greater or equal to the 1/5 event over a large territory at the same time. This is how the scatter of points in Fig. 18 for small headwater basins can be interpreted. It is well known that AM-series do not contain as many very high floods as PD-series. In many years the AM-value does not belong to the PDS population of extreme events. The same phenomenon is observed when comparing PDS and SPDS. For downstream observation points in the main river branches the events represented are almost identical in the two data sets. Moving to smaller and smaller basins the agreement disappears gradually, i.e. the events contributing to the extreme situation in the main rivers do not belong to the population of extreme events for the small basins. To complete the picture Fig 19 shows all data used as a background for constructing the regional frequency curve. It is striking how few of the most extreme values for small and moderate basin sizes that are present in the diagram in Fig. 18.

If it is so that the risk of flooding has increased and the main cause for this is higher floods we should then first look for phenomena that can influence the synchronicity in the timing of floods in headwaters. The most important component here is the scale of weather systems causing extreme floods: change in temperature over large areas in lowlands and mountains simultaneously creating snowmelt and/or intense precipitation over large areas. Are such large-scale weather systems more frequent now than before? Another factor of importance can be such a change in response times in headwaters and transport times in channels that the time of concentration became lower, which increases the chance of a simultaneous response of the whole drainage basin. It is out of the scope to address these questions here in depth. A visual analysis of the plotted long PDS series, their magnitude (Fig. 20a) and the day of the occurrence (Fig. 20b) of floods gives no indication of any major changes during the last 100 years for the Glomma River. There is a tendency for more frequent autumn floods in the Glomma branch during the last decade. This is in agreement with the recent conclusions of the effect of climate change on the hydrological regimes of Norwegian rivers (Krasovskaia and Sælthun, 1997).

An alternative methodology for streamflow frequency estimation that has gained wide popularity is the so-called derived distribution approach. The approach allows considering the knowledge about the hydrological processes generating streamflow, i.e. developing the chain of events in the runoff formation process that leads to a certain frequency of streamflow. Streamflow variables are related to precipitation data (which are better defined: longer record history, spatially more dense and more uniform), antecedent moisture conditions in the drainage basin and the basin response to a precipitation input. Eagleson (1972) was the first to use this approach for the derivation of flood frequency, later followed by Carlson and Fox (1976). The use of the Geomorphologic Unit Hydrograph (Rodriguez-Iturbe and Valdes, 1979) as a basin response model resulted in several studies on the topic of derived flood frequency distribution. Other examples are Hebson and Wood (1982), Diaz-Granados et al. (1984), Moughamian et al. (1987), Sivapalan et al. (1990) and Gottschalk and Weingartner (1998). The derived frequency distribution approach also plays a dominant role in studies of scaling of regional floods. Blöschl and Sivapalan (1995) provide an overview of the recent very large publication activity in this field.

The regional curves in Fig. 18 are derived purely from the observed data and no understanding of the physical processes behind has been utilised. Anyhow, it agrees with a general observation that large basins have a dampening effect on large floods. Is the derived distribution function approach an alternative to approach the problem of constructing regional frequency curves like the one shown in the figure? Would it allow predicting the influence of environmental changes on these regional frequencies? This approach is at present mainly focused on the scaling of the characteristics of the distribution of areal precipitation and in the response times of a basin. Both these factors were earlier pointed out to be of primary importance. In our opinion, especially an insight in the response times and the effect of environmental change on this time can be gained by this approach. The scaling problem, and the related topic of synchronicity in events, is more complicated. For a spring flood in the Glomma it is connected to the joint structure of the spatial fields of snow cover, precipitation, temperature and soil moisture over a large territory. Below some more features of this complexity, as reflected in the SPDS data set, are discussed.

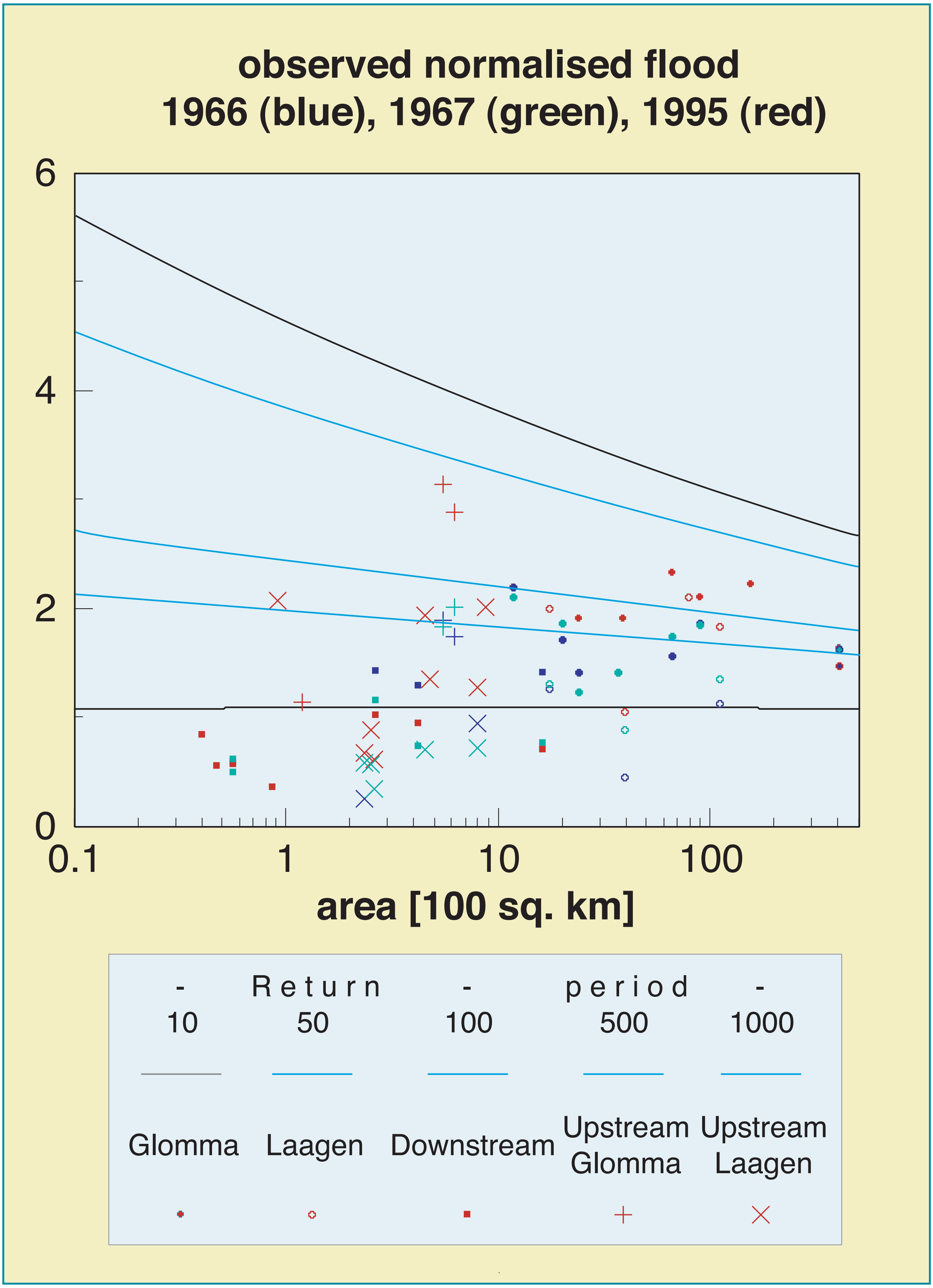

Figure 18. A regional frequency curve for the Glomma river for the normalised flood with respect to the mean flood. The scale factor is expressed as the area in km² divided by the area of a reference basin of 100 km². Empirical data from the floods in 1966, 1967 and 1995 are also shown.

5.3 Synchronicity in flood events

As a first step in such an analysis, it is very informative to study the annual hydrographs jointly for many stations. Fig. 20 shows the hydrographs for the flood 1995. It illustrates how the downstream events are gradually built up to form the hydrograph in the main river. The floods in the Glomma basin are extremely sensitive to the synchronicity between the two main branches: the Glomma and the Laagen. There is an apparent risk for floods that are much higher than those observed. This must be an important task for a continued analysis of the flood situation likely to occur in the Glomma. The spatial correlation between the most downstream station and those upstream in the SPDS data set give further insight in how the floods are linked (Fig. 22). There is at once a rather large drop in correlation between the largest basin and the second largest. It is again the effect of the large Mjøsa Lake. The correlation is then rather constant along the main branches of the Glomma and the Laagen. Also the upstream headwaters in the Glomma are well correlated. This is not the case for the headwaters in the Laagen. In many ways the constellation of points resembles that of the flood events in Fig.18.

The correlation coefficients give a picture of the average flood situation. What about the extreme floods situations? As an attempt to illustrate these, transition probabilities have been estimated for values above the median and the 75% and 90% quantiles i.e. the probability that if the flood at the downstream point is above the median (or other quantile) it is also above the median upstream. The result of this calculation is shown in Fig. 23. For comparison the theoretically calculated transition probabilities for a normal process with known correlation are also inferred in the figure. The tendency is rather clear (although there is some scatter in the data due to statistical errors, especially in the 90% values) that the events have larger transition probabilities than can be expected from the correlation (Fig. 22) for the events above the 75% and 90% quantiles. A conclusion that can be drawn is that the more extreme the downstream event the more correlated is it with the upstream events, i.e. the larger is the scale of the causing factors. This observation contradicts general models from probability theory that usually state that the more extreme the situation, the less is it correlated in space (compare Gottschalk, 1989).

5.4 The distribution function of flood stage at Nor.

At Nor there is available a short observation record of 10 years (1975-84). The maximum in 1995 is also available. The mean value and standard deviation of the annual maximum for this total of 11 years are 1564.4 and 541.0, respectively. The three parameters in the GEV distribution estimated by the l-moments are u=1313.9, α=333.9 and k=-0.150. The standard error in these local parameter estimates are calculated by so called jackknifing (Tukey, 1958) to 39.5, 20.9 and 0.270. The regional model gives an estimated mean value of 1599.7 and the following GEV parameters - u=1405.4, α=337.0 and k=-0.026. Table 4 shows the standard errors for these three parameters. We note that for the location parameter u the local estimate has the smallest estimated error. For the scale parameter a the local and regional estimates have almost identical errors. The shape parameter k, finally, is by far best estimated from the regional model, while the local estimate is very uncertain judging from the standard errors. The result makes sense. The short local series can help to improve an estimate of centrality and eventually scale. The form parameter, determining the shape of the tail for extremes, is to a small extent helped by the local short series. Instead the regional set of data is decisive for this parameter estimate. Utilising Bayesian principles the regional prior estimates can be updated by the local ones to derive a set of posterior parameter estimates by weighting in accordance with the inverse of the respective error variances. These posterior estimates are calculated to u=1318.7, α=335.5

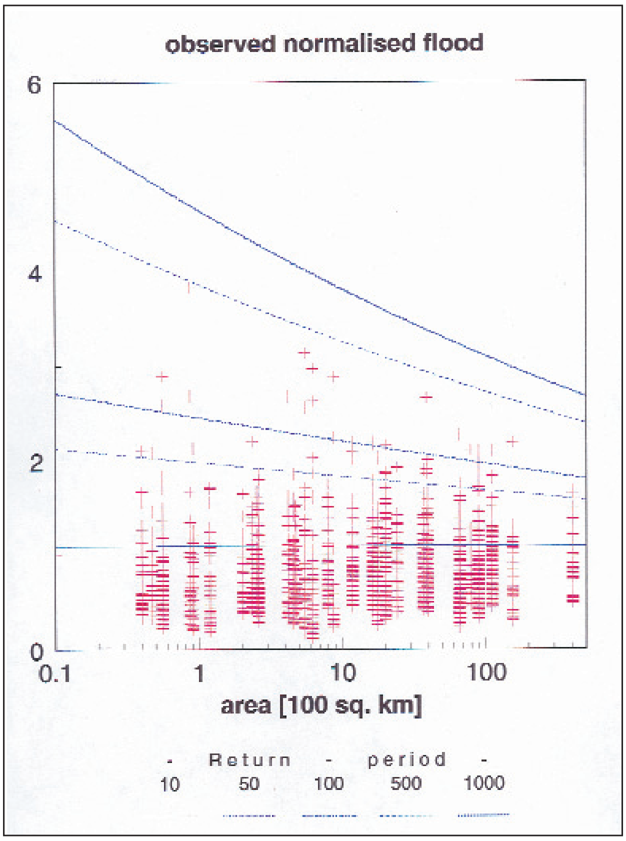

Figure 19. A regional frequency curve for the Glomma River for the normalised flood with respect to the mean flood. The scale factor is expressed as the area in km^2 divided by the area of a reference basin of 100 km^2. All empirical flood data used for the construction of the curves are also shown.

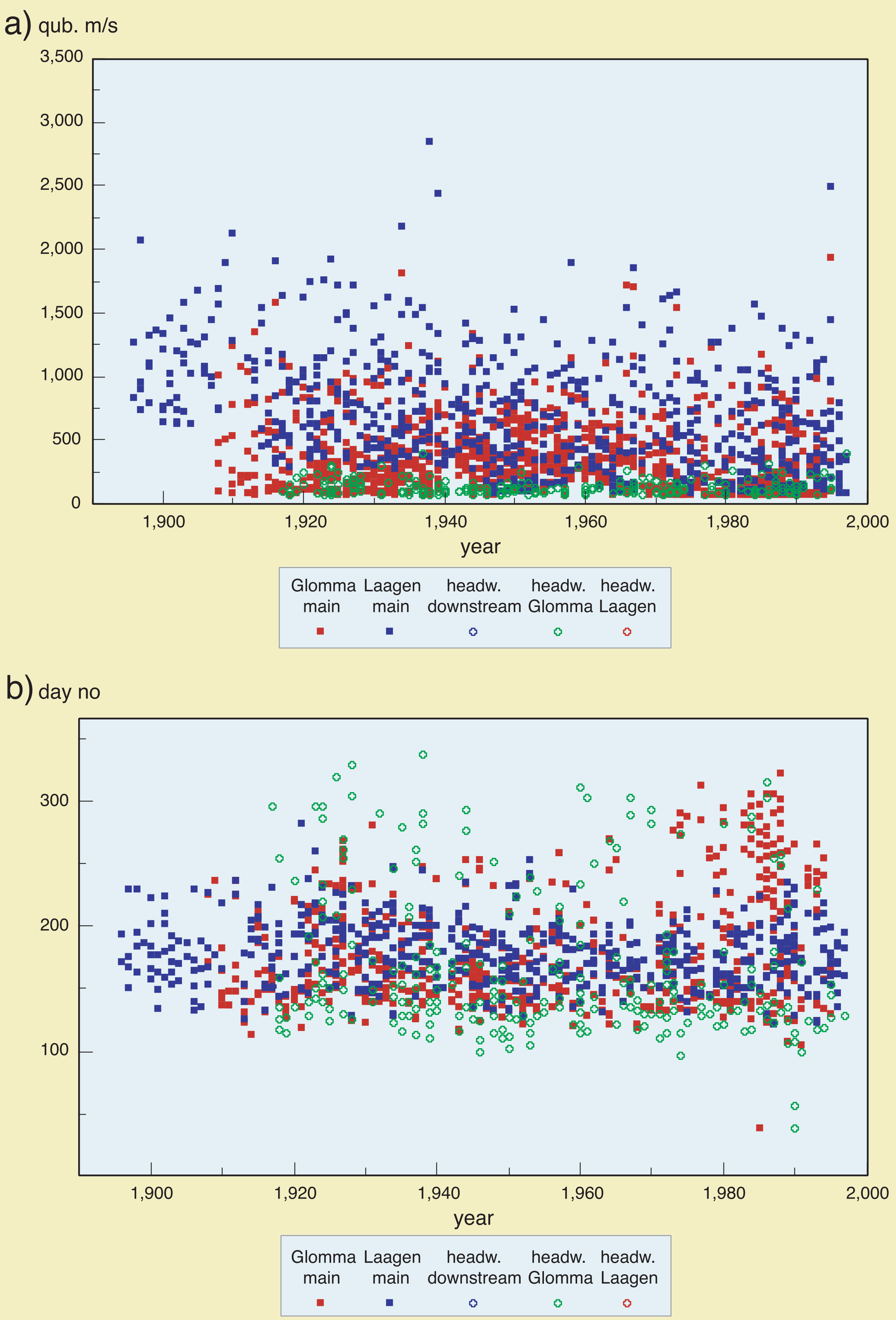

Figure 20. The magnitude of floods a) and the day of occurrence b) in long PD-series.

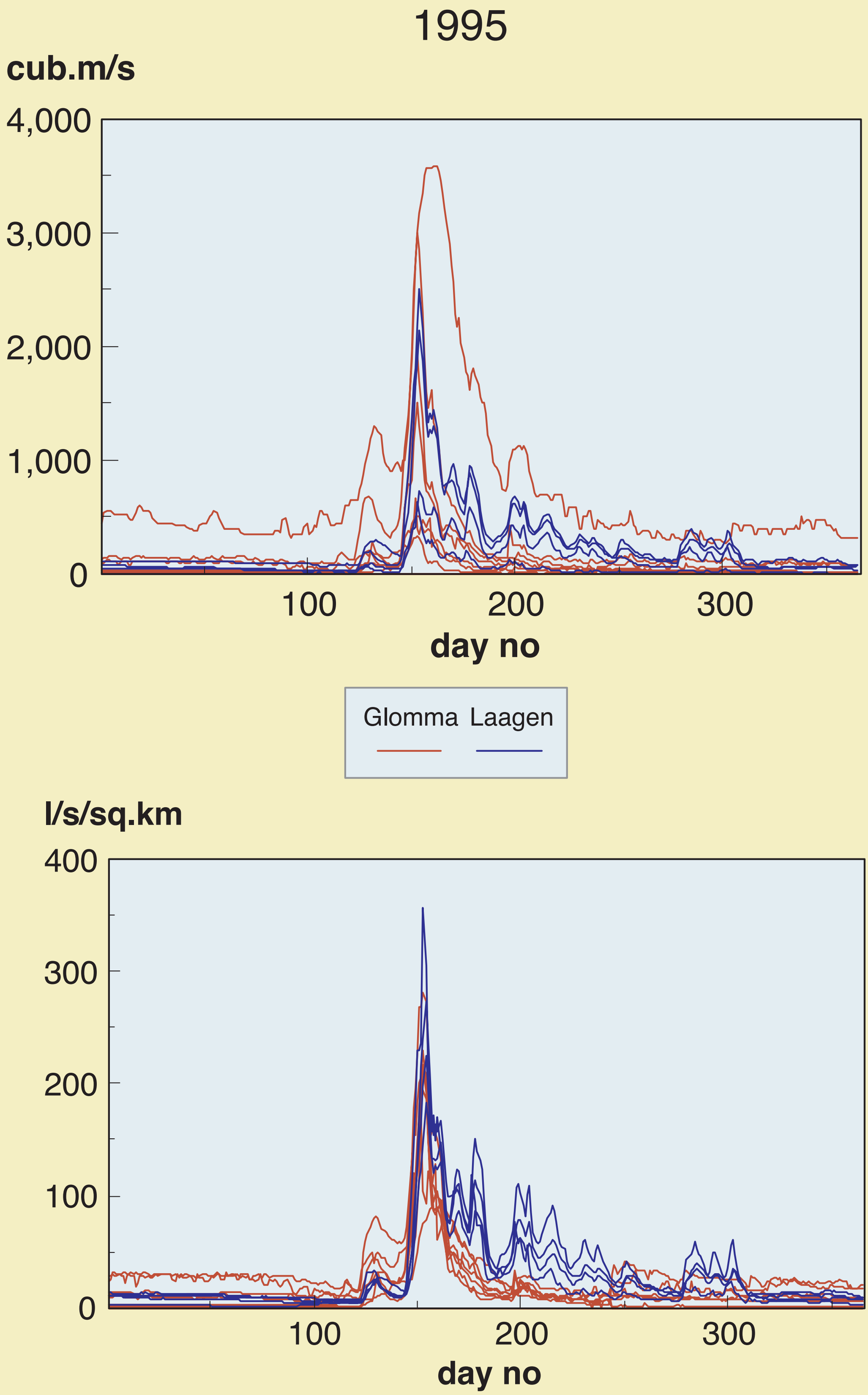

Figure 21. Annual hydrographs in the Glomma for 1995.

and k=-0.0289 and the corresponding standard errors are 38.0, 14.9 and 0.042. The errors in the estimates for the two first parameters are thus significantly reduced while the error of the third parameter k is not changed at all.

The posterior parameter estimates are those used in the following to determine the distribution function of discharge at Nor. Applying the transformation eq. (22) to the stage-discharge relation at Nor the distribution of river stage is derived. These two distribution functions are shown in Fig. 24.

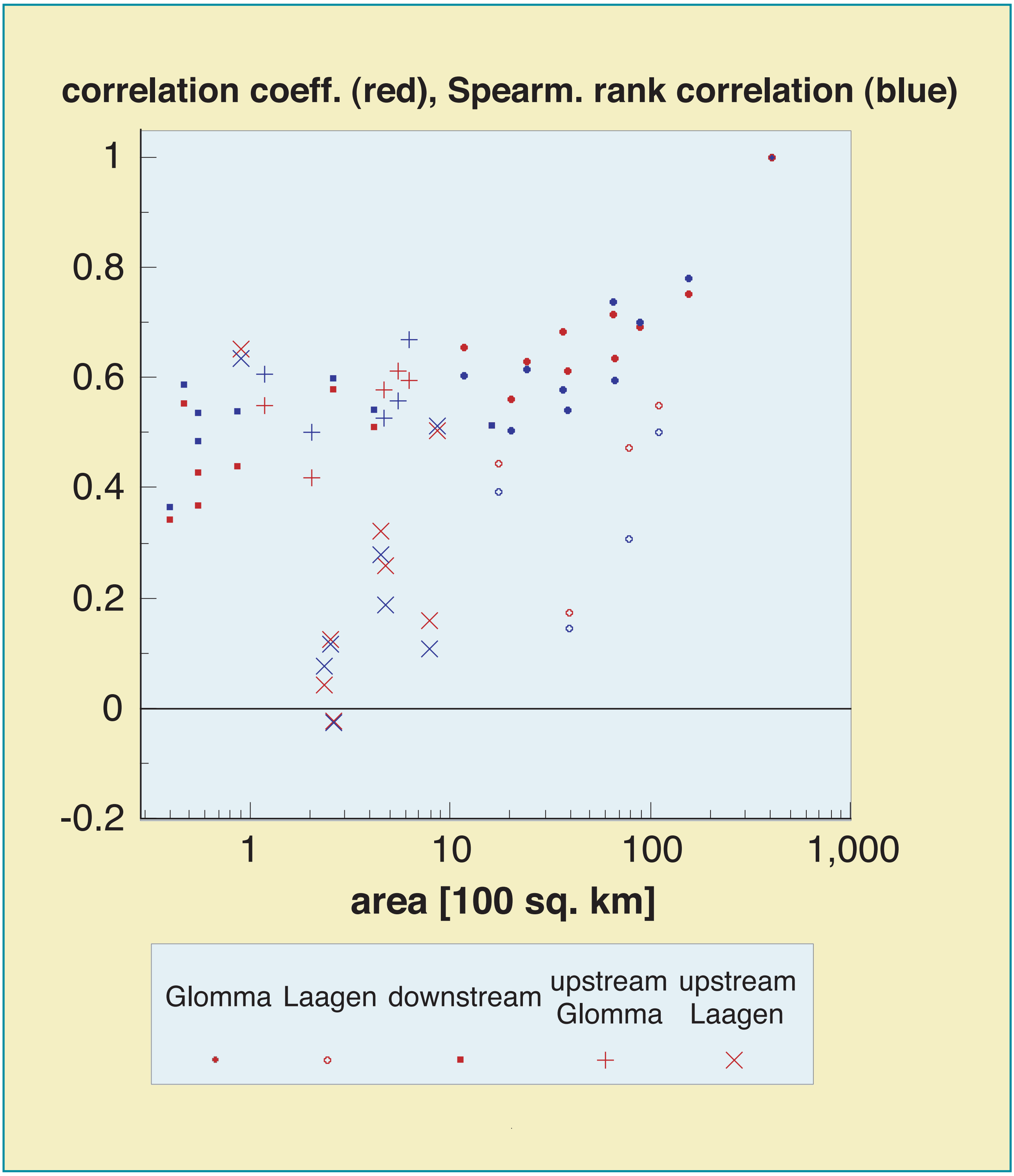

Figure 22. Spatial correlation between SPDS floods at Norbergsfoss (40221 km2) and at upstream stations.

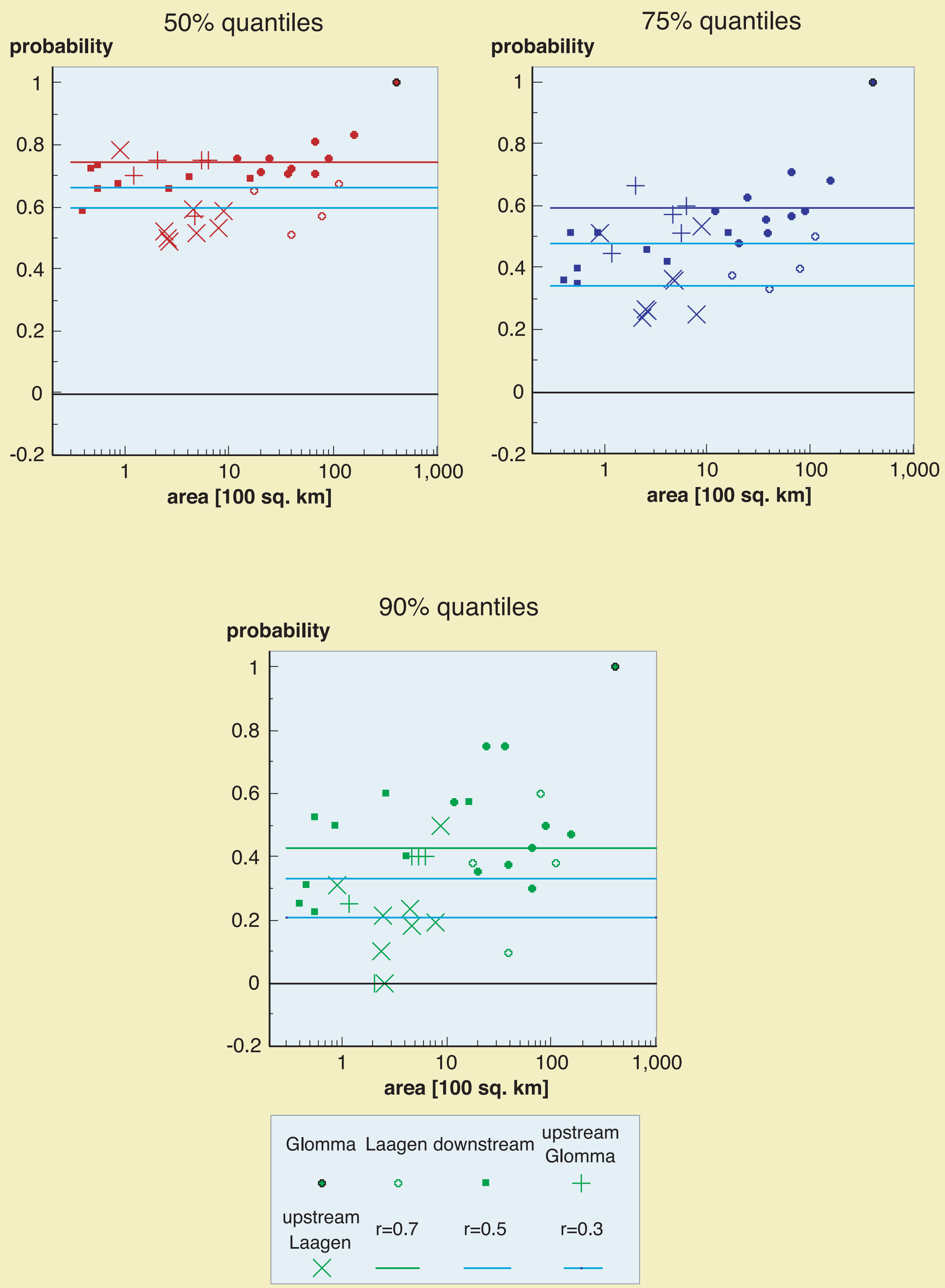

Figure 23. Spatial transition probabilities for the median, 75% and 90% quantiles between SPDS floods at Norbergsfoss (40221 km²) and at upstream stations.

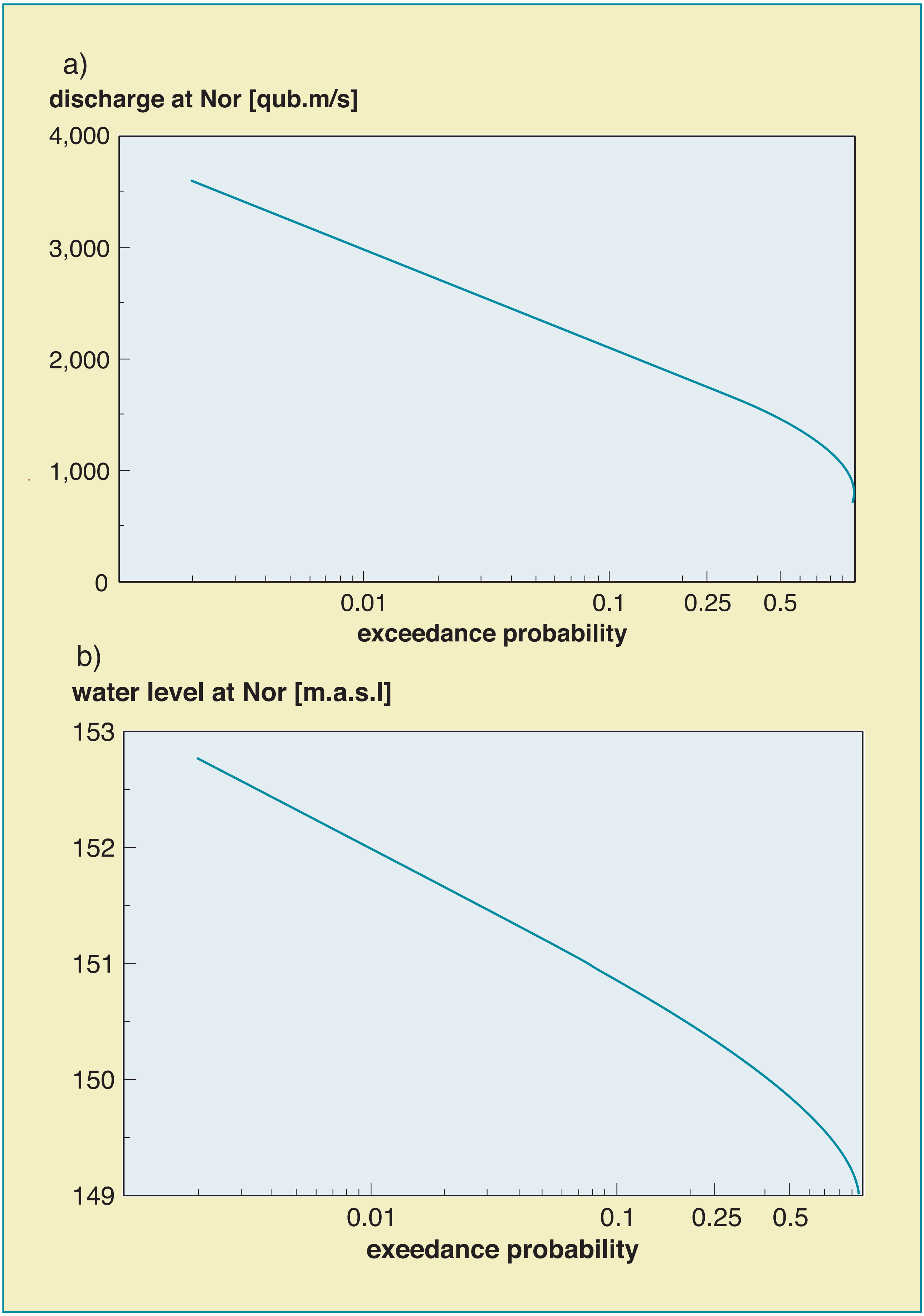

Figure 24. The distribution functions for discharge a) and flood stage b) at Nor.

5.5 Effect of uncertainty in regional frequency curve and stage-discharge relation

The fact that the parameters of the frequency curve contain errors as well as the parameters of the stage discharge relation results in errors in the estimated exceedance probability. Probabilities are defined over the interval [0,1], which also implies that the distribution of sampling errors of probabilities also are defined over this interval. This distribution is symmetric for probabilities around 0.5 but is more and more asymmetric towards 0 and 1, respectively. Errors are as a rule discussed with the normal distribution as a point of departure. In this case the standard error can easily be interpreted. The sampling distribution of estimates of probabilities is far from normal, especially for small exceedance probabilities. Cramér (1971) gives expressions for the estimation of confidence intervals around estimated probabilities when these arrive from a uniform distribution. Rasmussen (1991) derives expressions for the sampling distribution of estimated exceedance probabilities and its moments in case of a parent Gumbel distribution. There has not been possibility within the present project to study this problem in any depth. The analysis developed below is very preliminary and lacks a proper evaluation of the validity of the simplified approach of using truncated series expansions to estimate errors and bias in probability estimates.

The estimate of the probability of a water stage ζ is derived from the GEV distribution as:

$$\hat{p} = \exp\left[-\left\{1-\hat{k}\left(\hat{q}(\varsigma)-\hat{u}\right)/\hat{\alpha}\right\}^{1/\hat{k}}\right] \qquad (1)$$

The mean (bias) and the variance (standard error) of this regional exceedence probability estimator are obtained from a Taylor series approximation of eq. (1):

$$E\{\hat{p}\} = (p)_m + \tfrac{1}{2}\left(\frac{\partial^2 p}{\partial u^2}\right)_m Var\{\hat{u}\} + \tfrac{1}{2}\left(\frac{\partial^2 p}{\partial \alpha^2}\right)_m Var\{\hat{\alpha}\} + \tfrac{1}{2}\left(\frac{\partial^2 p}{\partial k^2}\right)_m Var\{\hat{k}\} + \tfrac{1}{2}\left(\frac{\partial^2 p}{\partial q^2}\right)_m Var\{\hat{q}\}$$

$$Var\{\hat{p}\} = \left(\frac{\partial p}{\partial u}\right)_m^2 Var\{\hat{u}\} + \left(\frac{\partial p}{\partial \alpha}\right)_m^2 Var\{\hat{\alpha}\} + \left(\frac{\partial p}{\partial k}\right)_m^2 Var\{\hat{k}\} + \left(\frac{\partial p}{\partial q}\right)_m^2 Var\{\hat{q}\} \qquad (2)$$

where $m = (u_i, \alpha_i, k_i, q(\varsigma))$ i.e. they are evaluated around the specific values of the parameters at site i and the discharge related to a certain river stage ζ. Both expressions contain four terms, one for each parameter and one for the stage-discharge relation. The standard errors for each of these have been evaluated above. To illustrate the role of uncertainties standard errors for two cases are evaluated - for the regional prior parameter estimates and for the posterior estimates when the local information is added. Fig. 25 shows the variation of these standard errors as a function of the probability p. In Table 5 the relative proportion of each of the four components is evaluated as a function of p.

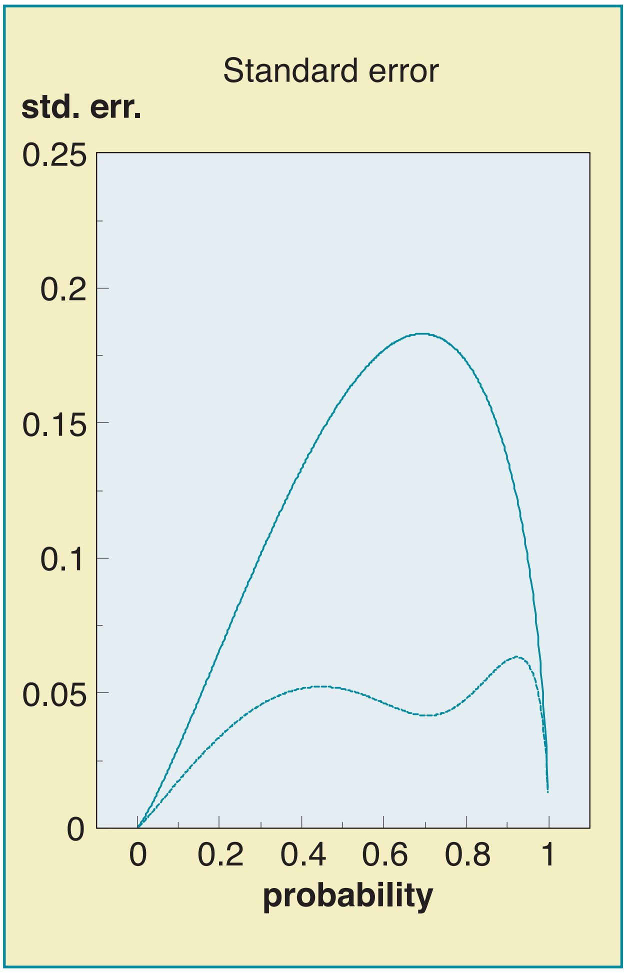

Figure 25. Estimated standard errors of probabilities for regionally estimated parameters (full line) and for those updated with local information (dashed line).

The general features of the graphs in Fig. 25 and the values in Table 5 make sense except for the fact that the role of the uncertainty due to the stage-discharge relation seems to be too dominant. This has to be looked into more carefully. It is of cause correct that the locally updated standard errors are reduced compared to the regional ones and at the same time the standard errors of the stage-discharge relation become more dominant. The uncertainty in the parameter of centrality is the most important one in the central part of the distribution. Towards the tails the scale and especially the form parameter take over this role. The uncertainty of the stage-discharge relation is lowest in the central parts and also increases towards the tails.

Table 5. Standard errors of estimated probabilities of the GEV distribution and the relative role (in percentage) of the uncertainties of parameters in the distribution of discharge and of the stage-discharge relation.

probability	std. error	u	α	k	q
regional (prior) parameters					
0.002	0.00028	31.4	5.0	3.0	60.7
0.010	0.00173	36.3	4.7	2.2	56.8
0.020	0.00383	39.4	4.5	1.9	54.3
0.050	0.01101	45.1	4.1	1.4	49.5
0.100	0.02420	51.5	3.6	0.9	43.9
0.200	0.05142	61.8	2.9	0.5	34.8
0.500	0.11502	88.9	0.8	0.0	10.2
0.800	0.12278	94.5	0.4	0.0	5.0
0.900	0.10393	70.5	2.2	0.2	27.0
0.950	0.08158	47.5	3.9	1.1	47.4
0.980	0.05397	28.1	5.2	3.3	63.4
0.990	0.03744	19.4	5.7	5.7	69.2
0.998	0.01432	9.1	5.9	12.8	72.2
locally updated (posterior) parameters					
0.002	0.00023	4.8	3.7	4.2	87.4
0.010	0.00139	5.9	3.6	3.4	87.1
0.020	0.00303	6.7	3.6	2.9	86.8
0.050	0.00836	8.3	3.6	2.3	85.8
0.100	0.01747	10.5	3.5	1.8	84.3
0.200	0.03384	15.1	3.4	1.1	80.4
0.500	0.05155	46.8	2.1	0.1	50.9
0.800	0.04796	65.5	1.4	0.0	33.0
0.900	0.06221	20.8	3.1	0.7	75.4
0.950	0.06080	9.1	3.6	2.0	85.4
0.980	0.04587	4.1	3.7	4.5	87.7
0.990	0.03342	2.6	3.6	6.9	86.8
0.998	0.01348	1.1	3.4	14.1	81.4

6. Risk estimation

Fig. 26 offers an illustration of the concluding results of this study, i.e. the damage distribution and the calculated risk of flooding for the study area. The curves and the risk estimates are derived according to the scheme shown in Fig. 9. The stage-damage curve (Fig. 15) and the distribution curve of river stage (Fig. 24b) are thus the background for constructing the damage distribution. The risk estimate is derived as the expected value of the damage distribution:

$$r = \int_0^\infty l f(l) dl \qquad (23)$$

Fig. 26 presents three cases. The first one, illustrated in Fig. 26a, shows the damage distribution for a hypothetical situation with no dikes. In such a case the curve is declining smoothly from high damages for low exceedance probabilities to moderate and low ones for high exceedance probabilities. The risk is estimated to 50 million Norwegian kroner (NOK). This value might seem low in relation to the very high damages of up to 1 billion NOK for the exceedance probability of 1/1000.

This reflects actually the criticism expressed by Thompson (1997) and others and quoted earlier in this report, who noted that the risk estimates give too much weight to very frequent but low damage causing events. The two curves in Fig. 26b consider the situation with the dikes existing at present. The curve for 1995 offers the damage description relevant for the year of the flooding. The curve for 1966 is a hypothetical one, where the number of buildings in the area has been reduced to their actual number that year. At this time the dikes were less extensive than in 1995 but this is not accounted for in the figure. The respective risk for the two cases are 4.9 million NOK and 3.7 million NOK. These figures are very low compared to the situation shown in Fig. 26a. This is obviously due to the fact that the damage is very low below the critical levels of the dikes, which, as it can be seen, represent approximately 1/100-flood. The damage for the flooding with lower exceedance is as high as this in Fig. 26a for the 1995-curve.

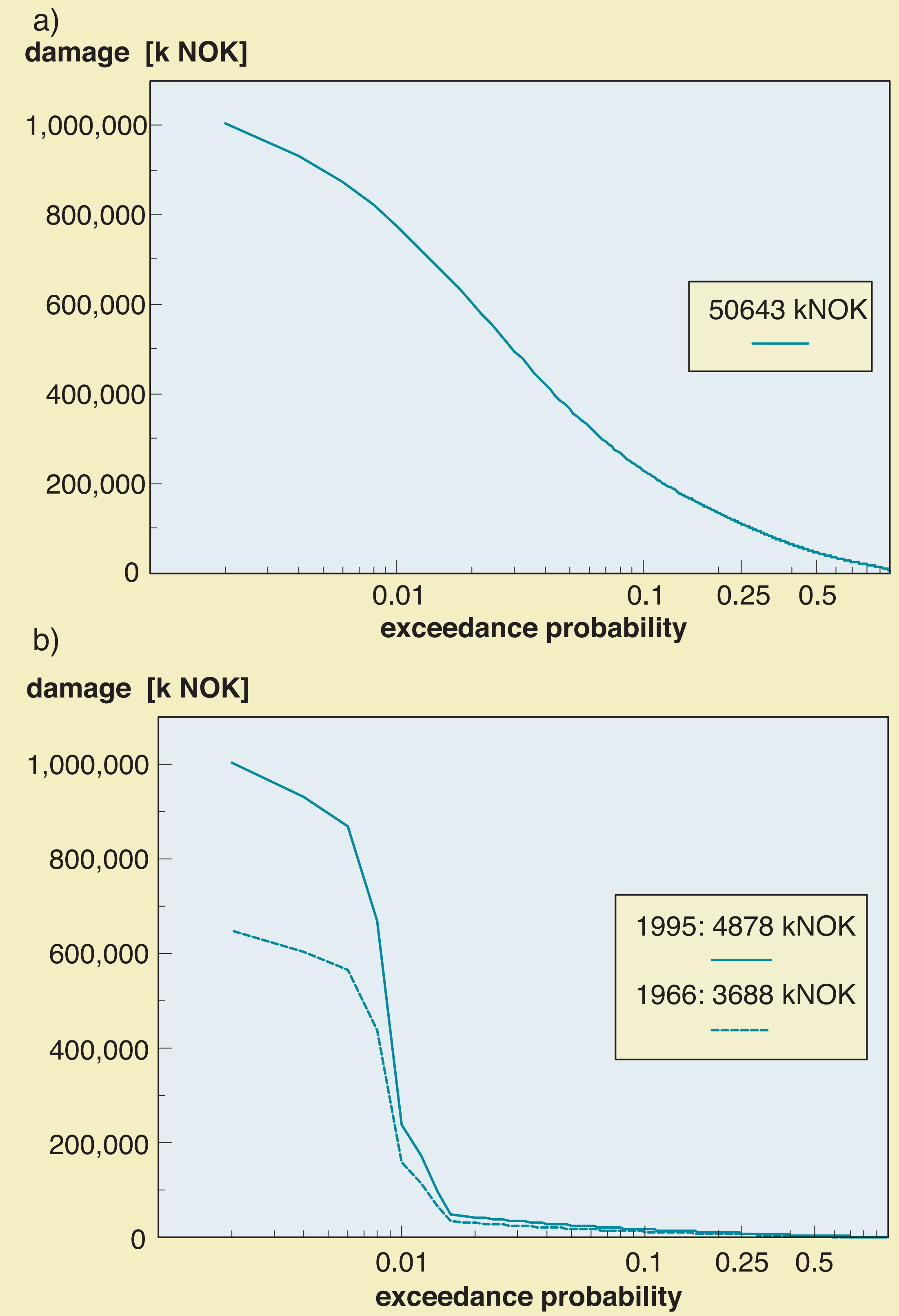

Figure 26. The distribution of damages for the floodplain upstream Nor. The full line in a) shows the case with the assumption that there are no physical obstacles preventing the river water from reaching a building at a certain altitude. The full line curve in b) is for the present (1995) situation when the height of the dikes constructed after the 1967 flood is accounted for. The dashed line shows a hypothetical curve for the number of buildings that existed in 1966.

7. Discussion and conclusions

A very preliminary unofficial estimate of the actual damage costs of the 1995 year flood for the Åsnes and Grue municipalities is 130 million NOK (Hallvard Berg NVE, personal communication). Of this total cost 80 million NOK is related to damage of buildings. This figure should be compared to the damage curve for 1995 in Fig. 26b. A damage of about 80 million NOK corresponds to a point on the curve where it starts to increase sharply at an exceedance probability of 1.5 % (i.e. a return period of 67 years). This would indicate that some dikes have started to be overtopped and areas protected by these were flooded. This is in agreement with what really happened. During the flooding the dikes were reinforced and topped with sand bags to withstand a higher river stage. This fact is of cause not reflected by the curve. The hypothetical damage that would have occurred without any reinforcements is probably significantly higher than the actual damage nearer to the 1% exceedance probability. It is a difficult task to in a formal way test and validate the damage distribution curves in Fig. 26. We can only conclude from this very rough comparison that the 1995 curve is in agreement with what really happened and that the values of damages are in a reasonable agreement. Here we should also point to the uncertainties in the estimate of the damage distribution curve. Some of these uncertainties are inherent to the problem and have to be accepted. Nature behaves in an unexpected way and surprises are common. Uncertainties due to limited amount of data are always a critical point. Economic constraints force us to accept that existing hydrologic and climatic observation networks cannot be significantly changed and thereby this part of the uncertainty cannot be reduced either. For other types of data (topographical, economic etc.) we can expect improvements towards a better resolution and larger samples. There are also several ways of improving the methodology developed here in order to obtain more reliable results.

Among the many factors that influence the risk of flooding only those classified as floodplain characteristics (economic activity, topography of objects (buildings), flood protection works, economic loss) play a significant role. This is clearly illustrated by the three curves in Fig. 26. The diagrams show how the risk changes with increased economic activity (compare the curves for the 1966 and 1995 year floods) and with the construction of dikes (compare the curve in a) with those in b)). Other factors like land use changes in upstream headwaters and non-stationarities in flood records have in comparison only a secondary influence in the risk estimation. Their contribution is difficult to separate from the different sources of statistical uncertainty.

The available data of damage costs related to the water level of flooded objects are quite unique for Norway and very valuable for this study. Anyhow, the data sample is rather small and it would be of great help with more data of this kind. The analysis has been concentrated to damage of buildings. The principles developed can, however, be applied to other type of objects linked to topography like roads, railways, agricultural land etc.. The number of damaged buildings and damage per building, respectively, need then to be replaced by length of damaged roads and damage cost per length unit etc..

The resolution in topographic data is of a vital importance for reliable estimates of risk of flooding. It is clearly shown here that such data taken from maps with 5 and 10 m contour intervals are not good enough and results are highly unreliable. Topographic data from maps with 1 meter contour intervals are acceptable but the uncertainty is still significant.

The flood line calculations have been rather superfluously treated in this study and a very simplified model has been used. Such calculations have been performed by other research groups in the HYDRA research programme. However, the results have not been available in time to be utilised here.

The methodology developed for establishing a regional frequency curve and for updating such a model with local information is possibly as far as one can reach at the present state-of-the-art to minimise the uncertainty in flood estimation at a specific site. The total uncertainty is still substantial and the part related to the choice of model needs further clarification. The total uncertainty can, however, only be significantly reduced by adding more observation points in space. The local updating procedure calls for the establishment of new observation to be sites at places where the present precision is considered unacceptable. The derived distribution function approach may offer better alternatives for the future and is a field open for new research initiatives. The present generation of conceptual models is not an alternative. Table 1 reveals that the uncertainty is 40%-100% higher when such models are used for flood estimation compared to a regional frequency curve.
A surprising result of the study is the relatively large role of the uncertainty in the stage-discharge curve in the total uncertainty of the estimate of a river stage with a certain exceedance probability. It is a fact that very rarely the discharges near to those extreme values that are in focus in the risk analysis of floods are measured and the stage-discharge curves are mostly extrapolated outside the range of observations. Anyhow the question needs further investigations.

The damage distribution curves have been established for a rather limited area. How would such curves look like for, say, the whole of the Glomma drainage basin? The problem is very complex. For each area with a potentiality for being flooded a damage distribution curve can be calculated with the methodology developed here and this is not problematic. The difficulties arise from the correct account of the synchronicity of flood events over large areas - how large is the area where we can expect a 100-year flood at the same time? The problem is related to another important question - how can information on upstream events be utilised to improve the precision in estimates of extreme floods downstream? For the Glomma river this question has special relevance as two equally large branches join together into one river reach. How do we estimate the frequency of extreme floods in the downstream Glomma knowing the frequency of extreme floods in the upstream branches of Glomma and Laagen? The analysis of the synchronicity of floods presented here is a first modest step to clarify these questions.

References

Ashkar, F. and Rouselle, J. (1981) Design discharge as a random variable: a risk study. Water Resources Research 17(3): 577-591.

Aven, T. (1992) Reliability and risk analysis. Elsevier Applied Sciences.

Bates, C.G. and Henry A.J. (1928) Forest and streamflow experiment at Wagon Wheel Gap, Colorado. Monthly Weather Review supplement No 30 74pp.

Berger, J.O. (1985) Statistical decision theory and Bayesian analysis. Second edition, Springer.

Blöschl, G. (1996) Scale and scaling in hydrology. Habilitationsschrift. Weiner Mitteilungen Wasser-Abwasser-Gewässer, Band 132. Herausgeber: O.Univ.Prof. Dipl.-Ing. Dr.Techn. Deiter Gutknecht, Technische Universität Wien, Institut für Hydraulik, Gewässerkunde und Wasserwirtschaft, Wien.

Blöschl, G. and Sivapalan M. (1995): Scale issues in hydrological modelling: a review, In: J.D. Kalma and M. Sivapalan (Editors), Scale Issues in Hydrological Modelling, Wiley, Chichester, 9-48.

Burrell, B. and Keefe, J. (1989): Flood risk mapping in New Brunswick: A decade review. Canadian Water Resources Journal 14:66-77.

Carlson, R.F., and Fox, P.A. (1976): Northern Snowmelt-Flood Frequency Model. Water Resources Research 12 (4):786-794.

Caspary, H.J. (1998) Regional increase of winter floods in southwest Germany caused by atmospheric circulation changes (abstract). Annales Geophysicae Part II Hydrology, Oceans & Atmosphere, Supplement II to Volume 16 p. C463.

Cramér, H. (1971) Mathematical methods of statistics. Princeton University Press, Princeton 1946 (12 printing 1971).

Dalrymple, T., Flood-frequency analysis. U.S. Geological Survey Water Supply Paper 1543-A, 80 pp, 1960.
Dawdy, D.R. (1961) Variation of flood ratios with size of drainage area. U.S. Geological Survey Professional Paper 424-C:C36.

Desbos, E. (1995) Qualification de la vulnérabilité du territoire face aux inondations. Rapport de D.E.A. "Conceptions en bâtiment et techniques urbaines", INSA Lyon, laboratoire Méthodes, Cemagref Lyon, 70p.

Diaz-Granados, M.A., Valdes, J.B. and Bras, R.L. (1984): A physically based flood frequency distribution. Water Resources Research 20(7):995-1002.

Eagleson, P.S., (1972): Dynamics of Flood Frequency. Water Resources Research, 8(4):878-898.

Engler, A. (1919) Einfluss des Waldes auf den Stand der Gewasser. Mitt. Schweiz. anst. für das Forsliche Versuchswesen 12, 626.

Erichsen, B. (1995) Frekvensanalyse av 1995 flommen i Glomma, Gudbrandsdals-lågen og Trysilelven. NVE Hydrologisk avd. Publikasjon Nr 23 39pp.

Francou, J. and Rodier, J.A. (1967) Essai de classification des crues maximales observées dans le mond. Cahiers ORSTOM, Série Hydrologie IV (3).

Galea, G. and Prudhomme, C. (1994) Notions de base et concepts utiles pour la compréhension et la modélisation synthétiques des régimes de crue des bassins versants au sens des modèles QdF. Revue des sciences de l'eau 10(1):83-101.

Gilard, O. (1998) Les bases techniques de la méthod Inondabilité. Cemagref Édition.

Gottschalk, L. (1989) Regional exceedence probabilities. Nordic Hydrology 20:201-214.

Gottschalk,L. and Sælthun,N.R. (1990) Large scale temporal variability and risk of design failure. (Abstract) Annales Geophysicae, EGS XV General Assembly, Copenhagen, 1990.

Gottschalk, L. and Krasovskaia, I. (1997) Climate change and river runoff in Scandinavia, approaches and challenges. Boreal Environment Research, 2(2): 145-162.

Gottschalk, L. and Weingartner, R. (1998) Distribution of peak flow derived from a distribution of rainfall volumes and runoff coefficient, and a unit hydrograph. Journal of Hydrology 208:148-162.

Gottschalk, L. and Weingartner, R. (1998) Scaling of regional floods - an L-moment approach. European Geophysical Society XXIII General Assembly Nice, 20-24 April. Abstract. European Geophysical Society, Annales Geophysical, Part II, Hydrology, Oceans and Atmosphere, Suppelment II toVol. 16.

Gupta, V.K., Mesa, O. and Dawdy, D.R. (1994) Multiplicative cascades and spatial variability of rainfall, river networks and floods. In: Rundle, J., Klein, W. and Turcotte, D. (Eds.) Reduction and predictability of Natural Disasters. SantaFe Institute, XXV, Addison-Wesley.

Gupta, V.K. and Dawdy, D.R. (1994) Regional analysis of flood peaks: multiscaling theory and its physical basis. In: Rosso, R., Peano, A., Becchi, I. and Bemporad, A. (Eds.) Advances in Distributed Hydrology, Water Resources Publications, Highland Ranch, CO, 147-168.

Gupta, V.K. and Dawdy, D.R. (1995) Physical interpretations of regional variations in the scaling exponents of flood quantiles. Hydrological Processes 9(3/4):347-361.

Gupta, V.K. and Waymire, E. (1996) Multiscaling properties of spatial rainfall and river flow distributions. Journal of Geophysical Research 95(D3):1999-2009.

Haan, C.T. (1977) Statistical methods in hydrology. The Iowa State University Press, Ames, Iowa 378 pp.

Handmer, J.H. (1983) Risk information for floodplain management, Discussion. Journal of Water Resources Planning and Management ASCE, 114:120-123.

Hebson, C. and Wood, E.F. (1982) A derived flood frequency distribution using Horton order ratios. Water Resources Research 18(5): 1509-1518.

Hosking, J.R.M. (1990) L-moments: Analysis and estimation of distributions using linear combinations of order statistics. Journal of the Royal Statistical Society B52: 105-124.

Hosking, J.R.M. and Wallis, J.R. (1993) Some statistics useful in regional flood frequency analysis. Water Resources Research 29(2): 271-282.

Jain, S.K., Yogararasin, G.N. and Seth, S.M. (1992) A risk-based approach for flood control operation of a multipurpose reservoir. Water Resources Bulletin 28(6): 1037-1043.

James, L.D. and Hall, B. (1986) Risk information for floodplain management. Journal of Water Resources Planning and Management ASCE, 112:485-499.

Jaeggi, M.N.R. and Zarn, B. (1990) A new policy in designing flood protection schemes as a consequence of the 1987 floods in the Swiss Alps. In W.R. White (ed.) International Conference of River Flood Hydraulics, Hydraulic Research Limited, John Wiley and Sons Ltd. pp 75-84.

Karlsson and Haimes (1988a) Risk based analysis of extreme events. Water Resources Research 22(1): 8-20.

Karlsson and Haimes (1988b) Probability distributions and their partitionings. Water Resources Research 22(1): 21-29.

Kite, G.W. (1977) Frequency and risk analysis in Hydrology. Water Resources Publications, Fort Collins, Colorado.

Krasovskaia, I. (1996) Stability of river flow regimes. Dr. Philos. thesis, Department of Geography, University of Oslo, Norway, Rapport No 5, Oslo.

Krasovskaia, I. and Sælthun, N.R. (1997) Sensitivity of the stability of Scandinavian river flow regimes to a predicted temperature rise. Hydr.Sci.J. 42 (5), 693-711

Krasovskaia, I., Gottschalk, L., Rodrigues, A. and Laporte, S. (1999) Dependence of the frequency and magnitude of extreme floods in Costa Rica on SOI. IAHS Publication no 255:81-89.

Kundzewicz, Z.W. (1998) Floods of the 1990s: Business as usual? WMO Bulletin 47(2): 155-160.

Kuusisto, E., Lemmelä, R., Liebscher, H. and Nobilis, F. (1994) Climate and water in Europe: some recent issues. WMO RAN Working group on hydrology, Helsinki.

Lambert, J.H. and Li, D. (1994) Evaluating risk of extreme events for univariate loss functions. Journal of Water Resources Planning and Management ASCE 120(3): 382-399.

Loucks, D.P., Stedinger, J.R. and Haith, D.A. (1981) Water resources systems planning and analysis. Prentice-Hall, Inc. N.J.

Lowrance, W.W. (1976) Of acceptable risk. William Kaufmann inc., Los Altos, California.

Mays, L.W. and Tung, Y.-K. (1992) Hydrosystems engineering and management. McGraw-Hill, Inc. New York.

Mitsiopolous, J., Haimes, Y.Y. and Li, D. (1991) Approximating catastrophic risk through statistics of extremes. Water Resources Research 27(6). 1223-1230.

Moughamian, M.S., McLaughlin, D.B. and Bras, R.L. (1987): Estimation of flood frequency: An evaluation of two derived distribution procedures. Water Resources Research 23(7):1309-1319.

Paine, J.D. and Watt, W.E. (1992): Flood risk mapping in Canada: 2. Compatible mapping. Canadian Water Resources Journal 17:139-151.

Parett, N.F. (1987) Bureau of Reclamation use of risk analysis. In Singh, V.P. (ed.) Application of frequency and risk in water resources. D. Reidel Publishing Co. Boston, Mass. 411-428.

Plate, E. J. (1998) Probabilistic design for flood protection structures. In Casale, R., Pedroli, G.B. and Samauels, P. (eds.) Ribamod, River basin modelling, management and flood mitigation, concerted action. Environment and climate programme. European Commission EUR 18019 EN: 43-56.

Rasmussen, N.C. (1981) The application of probabilistic assessment technology to energy technologies. Annual Rev. of Energy 6:123-138.

Rasmussen, P.F. (1991) On the sampling distribution of exceedance probabilities. In Ganulis, J. Water resources engineering risk assessment. NATO ASI Series Vol. G29: 91-96.

Rodda, J.C. (1976) Facets of Hydrology. John Wiley and Sons.

Rodda, J.C. (1995): Wither World Water. Water Resources Bulletin 31(1):1-7.

Rodriguez-Iturbe, I. and Valdes, J.B. (1979): The geomorphologic structure of hydrological response. Water Resources Research 15(6):1409-1420.

Rowe, W. D. (1979) Introduction to risk assessment. In: G. T. Goodman and W. D. Rowe "Energy risk management": 7-19, Academic Press.

Simonovic, S.P. and Mariño, M.A. (1981) Reliability programing in reservoir management 2. Risk loss functions. Water Resources Research 17(4): 822-826.

Simonovic, S.P. (1997) Risk in sustainable water resources management. In: D. Rosbjerg, N-E. Boutayeb, A. Gustard, Z. W. Kundzewicz and P. F. Rasmussen "Sustainability of water resources under increasing uncertainty", pp.3-17, IAHS Publ.240.

Sivapalan, M.,Wood, E.F. and Beven, K.J. (1990): On hydrologic similarity 3. A dimensionless flood frequency model using a generalized geomorphologic unit hydrograph and partial area runoff generation. Water Resources Research 26(1):43-58.

Smith, J. (1992) Representation of basin scale in flood peak distributions. Water Resources Research 28(11):2993-2999.

Springer, M.D. (1979): The algebra of random variables. John Wiley & Sons.

Starr, C. (1969) Social benefit versus technological risk. Science 165 (3899): 1232-1238.

Stedinger, J.R. (1997) Expected probability and annual damage estimation. Journal of Water Resources Planning and Management ASCE 123(2): 125-135.

Tang, W.H., Mays, L.W. and Yen, B.C. (1975) Optimal risk-based design of storm sewer networks. Journal of Environmental Engineering ASCE 103(3): 381-398.

Thompson, K.D., Stedinger, J.R. and Heath, D.C. (1997) Evaluation and presentation of dam failure and flood risk. Journal of Water Resources Planning and Management ASCE 123(4): 216-227

Tung, Y.-K. and Mays, L.W. (1981) Optimal risk-based design of flood levee systems. Water Resources Research 17(4): 843-852.

Tukey, J.W. (1958) Bias and confidence in not-quite large samples. (Abstract) Ann. Math. Stat. 29:614.

Tveito, O.E. (1993) A regional flood frequency analysis of Norwegian catchments. Dep. of Geophysics, University of Oslo, Report No 86.

Vogel, R.M. and Fennessay, N.M. (1993) L-moment diagrams should replace product-moment diagrams. Water Resources Research 29:1745-1752.

Wathne, M. (1998) Samfunnskostnader på grunn av flomskade i vassdrag. SINTEF Rapport, Trondheim.

Watt, W.E. and Paine, J.D. (1992): Flood risk mapping in Canada: 1. Uncertainty considerations. Canadian Water Resources Journal 17:129-138.

WMO (1995): The global climate system, Climate system monitoring June 1991-November 1993. WMO-No 819, ISBN 92-63-10819-6.

Yevjevich, V. (1977) Risk and uncertainty in design of hydraulic structures. In Gottschalk, L., Lindh, G. and de Maré, L. (eds.) Stochastic Processes in Water Resources Engineering. Water Resources Publications, Fort Collins, Colorado ??-??.

Yongquan, W.(1993) Solar activity and maximum floods in the world. In: Kundzewich, Z.W., Rosbjerg, D., Simonovic, S.P. and Takeuchi, K. (eds.) Extreme hydrological events: Precipitation, Floods and Drought. IAHS Publ. 213:121-127.

Tidligere utgitt i HYDRA-serien

Flomdemping, flomvern og flomhandtering (F)

F01 Analyse av lange flomserier.
Lars Andreas Roald, NVE.

F02 Estimating the mean areal snow water equivalent from satellite images and snow pillows.
Thomas Skaugen, NVE.

F03 Modellstudie av reguleringens flomdempende effekt i Gudbrandsdalslågen.
Magne Wathne og Knut Alfredsen, SINTEF.

F04 Effekt av vassdragsreguleringer i Glomma og Lågen på stor flom.
Jens Kristian Tingvold, Glommens og Laagens Brukseierforening (GLB).

Miljøvirkninger av flom og flomforebyggende tiltak (Mi)

Mi01 Miljøkonsekvenser av flom - flom og vannkvalitet.
Bjørn Faafeng, Espen Lydersen, Gøsta Kjellberg, Vilhelm Bjerknes, NIVA.

Mi02 Virkning av flom på vannlevende organismer.
Åge Brabrand, John E. Brittain, Ketil Sand, Per Aass, UiO
Gunnar Halvorsen, Kjetil Hindar, Arne Jensen, Bjørn Ove Johnsen, NINA
Jo Vegar Arnekleiv, Dag Dolmen, NTNU
Bjørn Rørslett, NIVA
Jan Henning L'Abée-Lund, NVE.

Mi03 Miljøeffekter av flomforebyggende tiltak - en litteraturstudie.
Torbjørn Østdahl, Trond Taugbøl og Børre Dervo, Østlandsforskning.

Mi04 Miljøtilpasninger ved eksisterende og nye flomsikringstiltak – en litteraturstudie.
Torbjørn Østdahl og Trond Taugbøl, Østlandsforskning.

Naturgrunnlag og arealbruk (N)

N01 Naturlige magasineringsområder.
Bjørn Follestad, Norges geologiske undersøkelse
Noralf Rye, Geologisk institutt, UiB.

N02 Naturgrunnlag og arealbruk i Glommas nedbørfelt.
Arne Grønlund, Jordforsk.

N03 Endringer i landbrukets arealbruk i Glommas nedbørfelt.
Arne Grønlund, Arnor Njøs og Bjørn Kløve, Jordforsk.

N04 LANDPINE - en hydrologisk modell for simulering av arealbruksendringers innvirkning på avrenningsforhold.
Trond Rinde, SINTEF - Bygg og miljøteknikk.

Skaderisikoanalyse (R)

R02 Samfunnskostnader på grunn av flom i vassdrag.
Magne Wathne og Morten Skoglund, SINTEF
Hans Olav Eggestad, Jordforsk.

Tettsteder (T)

T01 Betydningen av lokal-/total overvannsdisponering (LOD/TOD) på flommer.
Svein Endresen, Siv.ing. Svein Endresen AS.

T03 Lokal og total overvannsdisponering (LOD/TOD) - Beskrivelser av anlegg, erfaringer mm.
Svein Endresen, Siv.ing. Svein Endresen AS.

T04 Skadereduserende kommunaltekniske tiltak med tanke på flom.
Svein Endresen, Siv.ing. Svein Endresen AS og Oddvar Lindholm, NLH.

Kontaktpersoner

formann i styringsgruppen:
Ola Skauge
Tlf. 73 58 05 00
E-post: ola.skauge@dirnat.no

programleder:
Arnor Njøs
Jordforsk
Tlf. 64 94 81 70 (Jordforsk)
Tlf. 22 95 90 98 (NVE)
E-post: arnor.njos@jordforsk.nlh.no
E-post: xarn@nve.no.

naturgrunnlag og arealbruk:
Arne Grønlund
Jordforsk
Tlf. 64 94 81 09
E-post: arne.gronlund@jordforsk.nlh.no

Noralf Rye
Universitetet i Bergen
Tlf. 55 58 34 98
E-post: noralf.rye@geol.uib.no

tettsteder:
Oddvar Lindholm
Norges Landbrukshøgskole
Tlf. 64 94 87 08
E-post: oddvar.lindholm@itf.nlh.no

flomdemping, flomvern og flomhandtering:
Dan Lundquist
Glommens og Laagens
Brukseierforening
Tlf. 22 54 96 00
E-post: post@glb.no
E-post: danlund@sn.no

skaderisikoanalyse:
Nils Roar Sælthun
Norsk institutt for vannforskning
Tlf. 22 18 51 21
E-post: nils.saelthun@niva.no

miljøvirkninger av flom og flomforebyggende tiltak:
Olianne Eikenæs
Norges vassdrags- og energidirektorat
Tlf. 22 95 92 24
E-post: oli@nve.no

databaser og GIS:
Lars Andreas Roald
Norges vassdrags- og energidirektorat
Tlf. 22 95 92 40
E-post: lars.roald@nve.no

modellarbeid:
Ånund Killingtveit
Norges teknisk-naturvitenskaplige universitet
Tlf. 73 59 47 47
E-post: aanund.killingtveit@bygg.ntnu.no

programadministrasjon:
Olianne Eikenæs
Norges vassdrags- og energidirektorat
Tlf. 22 95 92 24
E-post: oli@nve.no
Hjemmeside: http://www.nve.no

Per Einar Faugli
Norges vassdrags- og energidirektorat
Tlf. 22 95 90 85
E-post: pef@nve.no

Norges
vassdrags- og
energidirektorat

NVE

Kontoradresse: Middelthuns gt. 29

Postadresse: Postboks 5091 Maj. 0301 Oslo

Forsidefoto: Lauta i Åsnes kommune, juni 1995. Storflommen førte til brudd i flomverket og store skader på bygninger. Foto: Hallvard Berg, NVE.
Layout: ABC Visuell Kommunikasjon. Omslag: Gazette. ISBN: 82-410-0395-1